Master's Thesis

Information-based path planning for source term estimation using an unmanned aerial vehicle: algorithms and experiments

Seulbi An

Department of Mechanical Engineering
(Mechanical Engineering)

Ulsan National Institute of Science and Technology

2021

Information-based path planning for source term estimation using an unmanned aerial vehicle: algorithms and experiments

Seulbi An

Department of Mechanical Engineering
(Mechanical Engineering)

Ulsan National Institute of Science and Technology

Information-based path planning for source term estimation using an unmanned aerial vehicle: algorithms and experiments

A thesis/dissertation submitted to
Ulsan National Institute of Science and Technology
in partial fulfillment of the
requirements for the degree of
Master of Science

Seulbi An

12/10/2020 of submission

Approved by

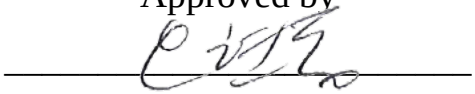

Advisor
Hyondong Oh

Information-based path planning for source term estimation using an unmanned aerial vehicle: algorithms and experiments

Seulbi An

This certifies that the thesis/dissertation of Seulbi An is approved.

12/10/2020 of submission

Signature

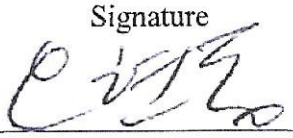

Advisor: Hyondong Oh

Signature

Cheolhyeon Kwon

Signature

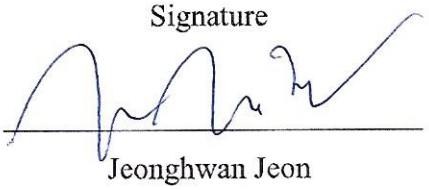

Jeonghwan Jeon

Abstract

Searching and estimating source information such as the location and release rate, called a source term, have many applications across environmental, medical, and security domains. For autonomous source search and estimation in a turbulent environment, this thesis presents two information-theoretic search strategies. Firstly, Gaussian mixture model (GMM) based infotaxis, termed as GMM-Infotaxis, is presented. The GMM is used to determine the action candidates for the next best informative sampling position in a continuous domain by appropriately clustering possible source locations obtained from the particle filter, compared with Infotaxis using discrete action candidates. This facilitates the better trade-off between exploitation and exploration for search, resulting in more efficient search and better estimation performance. However, GMM-Infotaxis has limitations in complex environments with many obstacles such as urban area, as this approach only predicts one step ahead action and the obstacles prevent efficient search. To address this problem, Infotaxis combined with the Rapidly-exploring Random Trees (RRT) is proposed and termed as RRT-Infotaxis. By introducing new utility function which is designed to maximize entropy reduction and minimize searching path at the same time, RRT-Infotaxis has advantage of searching efficient path in obstacle-rich environments. With proposed utility function, this approach is designed not only to avoid obstacles but also to sample the next best sampling positions considering several steps ahead in a continuous domain. Numerical simulations for both strategies, GMM-Infotaxis and RRT-Infotaxis, are implemented to prove the enhanced performance compared to the conventional Infotaxis. Numerical simulations show that in an open space the performance of GMM-Infotaxis is better than the conventional Infotaxis and in various urban environments RRT-Infotaxis outperforms both original Infotaxis and GMM-Infotaxis. Besides, real outdoor flight experiments using a multirotor UAV in an open space for GMM-Infotaxis are conducted. It shows the superior performance of the GMM-Infotaxis compared with the original Infotaxis method.

Contents

List of Figures

I Introduction

1.1 Background and Motivation

There are a large number of emergency situations from chemical biological or radiological material release into the atmosphere. In these situations, estimation of the source origin and release rate, called a source term, in a timely and accurate manner is one of the most important issues [1]. However, in highly non-linear and turbulent environments, sensing cues are often fluctuating, intermittent, or even absent. Another main difficulty arises from the dispersion phenomenon [2] triggered by irregular movements of airflow which are diffusion and advection or another unexpected event. To address these issues, research fields related to source term estimation using mobile sensors with various searching strategies have become popular over the last decade [1, 3–11]. Especially, Information-theoretic approach has an advantage in non-linear and turbulent environments. In these environments, sensing ques are not fine gradient so that the measurements toward the location of the source. Thus, assuming fine gradient condition does not fit in the real situation. Information-theoretic approach is designed to work in such conditions. It utilizes entropy, (i.e., uncertainty) and estimates source term in Bayesian framework using dispersion model, sensor model, and measurements. [8, 9, 12]. However, in most of the information-theoretic search algorithms [7–11, 13], the maneuver of the mobile robot is limited to cardinal directions. As the mobile robots select their next informative sampling position among the grid-based action candidates in a discrete space, they are likely to miss a chance to find the optimal maneuver. Increasing the number of discrete action candidates might improve the performance, however, this would also increase the computational load, making the algorithm intractable in real-time. In [11], when estimating the source term, the particle filter is utilized in a continuous domain. However, the maneuver of the mobile agent is still limited to neighboring grid points. Furthermore, there are lack of studies considering obstacles. There are some researches related to source localization in environments with obstacles [14–19]. However,

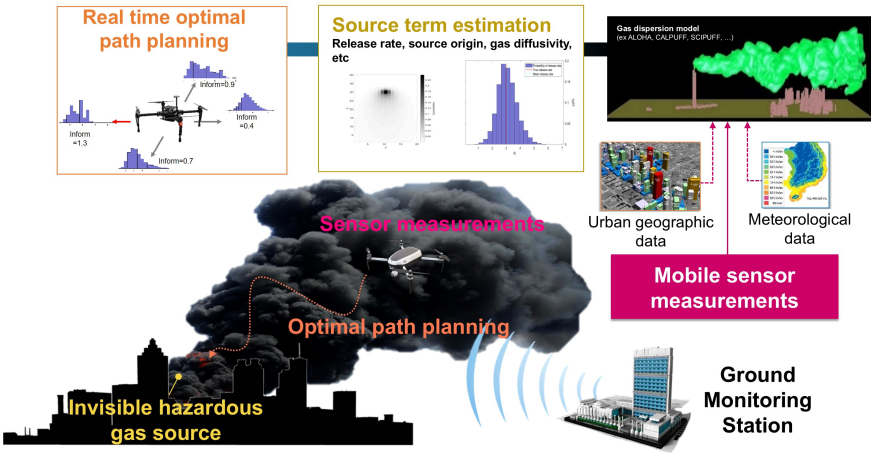

Figure 1: Concept of the source term estimation with a mobile agent.

even in these studies, the maneuver of the mobile agents are limited in grid points and affected by the size of the grid, (i.e., map resolution). Designing proper path plan of efficient source term estimation is still challenging due to the complex nature of the source dispersion not only in open area but also in obstacle environments. In this regards, planning efficient path for the mobile agent in open or complex environments is critical and necessary to deal with fast and efficient source term estimation in emergency situations.

1.2 Related Work

Autonomous source search strategies are widely employed in many kinds of tasks to declare the source by collecting cues or information with mobile sensors [1,3]. Many source term estimation algorithms are suggested, which could be largely categorized as gradient-based, bio-inspired, and information-theoretic methods [3]. In gradient-based methods, researchers assume a smooth concentration gradient of a source along the wind direction. A mobile robot exploits sensing cues with respect to the concentration gradient and wind direction [20]. However, this method is restricted to well-defined continuous concentration gradient fields. The structure of real plumes does not generate the fine gradient, so assuming the concentration field to be continuous and the gradient pointing towards the source is far from reality.

Bio-inspired methods are a strategy to guide the robots to the source location by imitating the behavior of living creatures such as moth or bacteria [4, 5]. It does not rely on gradient information but follows certain rules. For instance, it performs surge (going opposite to the wind) until missing the plume and cast (going across the wind by swinging with the increasing amplitude) to detect the plume again. However, these algorithms have a limitation to implement in reality. The sensing ability and locomotion of robots are far from those of real living creatures [5]. Furthermore, they do not utilize the prior information about the environment or the dispersion model even though this information is useful for unexplored areas [6].

Lastly, information-theoretic methods utilize the environment information in the form of entropy deducted from the sensor measurements and prior knowledge. Basically, these methods are based on the Bayesian framework to estimate the source term with the dispersion model, sensor model, and measurements. The representative example of the information-theoretic search algorithm called 'Infotaxis' was proposed by Vergassola et al. [7]. It was one of the first studies to apply the information-theoretic search strategy to various source search problems. The Infotaxis approach guides the mobile agent towards maximizing the entropy reduction. Recently, several source search algorithms based on Infotaxis strategies have been developed because of its robustness in realistic turbulent plume environments with noisy measurements [7–11, 13].

In most of the information-theoretic search algorithms [7–11,13], the maneuver of the mobile robot is limited to its neighboring grid points (in general, up, down, left, and right directions) due to the significant computational load in computing the predictive entropy at each point. However, as the mobile robots select their next informative sampling position among action candidates in a discrete space, they are likely to miss a chance to find the optimal maneuver.

Although increasing the number of discrete action candidates or finding optimal path/trajectory optimization [21–24] might improve the performance, this would also increase the computational load significantly, making the algorithm intractable in real-time. In [11], when estimating the source term, the particle filter is utilized in a continuous domain. However, the maneuver of the mobile agent is still limited to neighboring grid points.

Furthermore, all of the studies described above assume the source search mission is conducted in an open space. However, in real situation, the searching environment usually contains buildings or barriers which affect on the dispersion phenomena and hinder search process of the mobile agent. Several works covering complex environments have been studied in [14–19]. Ristic et al. [16, 17] assumed the environment as a grid map and obstacles are located at the 2-D lattice points, so that only passable links are remained. Yong Zhao et al. suggested source search strategy utilizing Entrotaxis [9] combined with obstacle bypassing strategy termed as Entrotaxis-Jump [18]. The same research group suggested hybrid strategies, Infotaxis and Entrotaxis with obstacle avoidance mechanism, when the map environment was not known in prior [19]. Although those studies are adequate with some environments filled with obstacles, those approaches are also affected by the obstacle configurations and grid sizes. Furthermore, especially in obstacle-rich environments, usually local optima occurs under constrained conditions. Due to these issues, limited maneuver of the mobile agent decreases the performance of the source search process in practical situations. Also, in obstacle-rich environments, considering long-term future state is needed. Therefore, source term estimation strategy in a continuous domain in open or the environments with the obstacles is needed.

1.3 Contribution of the Thesis

To address the above issues, this thesis first proposes an information-theoretic source search algorithm using the Gaussian mixture model (GMM) to suggest the admissible action candidates for the mobile agent in a continuous space. As this builds upon the discrete action space-based Infotaxis strategy [8], we term our proposed approach as GMM-Infotaxis. Similar to the previous work [8], the particle filter [25] is adopted for estimating the source term because of the high non-linearity of the real plume model. The particle filter not only updates the probability map at each iteration but also is utilized for generating the next best sampling position candidates. The more particles are gathered around a certain position, the more likely there might be a source nearby. To make use of this characteristic, the GMM is adopted where the potential source terms (i.e particles) are clustered using the estimated source location of the particle filter by the GMM, and its mean and variance information is utilized in determining the next best sampling position. Since the original Infotaxis approach is known to be biased toward exploration rather than exploitation [26], the proposed algorithm is designed to improve the exploitation property by selecting the sampling position candidates using the GMM that uses prior knowledge. Besides, we introduce the switching process depending on the variance of the source term estimation to utilize the benefit of both Infotaxis and GMM-Infotaxis algorithms;

when the agent has little information of the source (i.e. high variance of the GMM), the original Infotaxis is used for a better exploration and GMM-Infotaxis is used when the agent has enough information of the source for better exploitation. To the best of the author's knowledge, this is the first algorithm for autonomous mobile searchers to estimate the source term using the information-theoretic method in a continuous search rather than a grid (i.e discrete) domain. The comparison studies between original Infotaxis and GMM-Infotaxis methods are conducted in numerical simulations and real outdoor flight experiments.

However, in environments with obstacles, GMM action candidates may lead the mobile agent to wrong area as the candidates are blocked by the obstacles. Besides, only considering the next one step ahead is not appropriate in complex environments. For example, if the mobile agent only considers one step, it may move around the same region trapped by the local optima especially at the corner of the obstacle. To resolve this issue, a new source search strategy combined with Rapidly-exploring Random Trees (RRT), termed as RRT-Infotaxis, is proposed. This strategy also takes action candidates in a continuous domain. However, thanks to the nature of RRT, generated action candidates are in an obstacle free domain. Also, by considering generated path as long term source search process, RRT-Infotaxis has advantage of avoiding local optima. Besides, to balance exploration and exploitation in obstacle-rich environments, a new utility function is introduced which is a combination of maximizing entropy reduction and minimizing searching path derived by the A* algorithm.

The main contribution of the thesis is threefold. First, with the GMM and RRT, the proposed algorithms generate the next best informative sampling position in a continuous domain. Second, they secure the right balance between exploration and exploitation. Lastly, we validate the feasibility and superior performance of the proposed approaches with numerical simulations and real experiments. In particular, the superior performance of GMM-Infotaxis compared to the conventional Infotaxis is proven by real outdoor flight experiments using a multirotor UAV. The experiments that simultaneously conduct real-time source estimation and information-theoretic search using UAVs outdoors are rare since the wind flow is quite unpredictable and it is generally difficult to pick up the gas concentration in a large open area using a conventional gas sensor on-board the multirotor UAV. Although some recent studies have conducted source search experiments with actual plumes [27–30], those studies are conducted under the controllable wind flow conditions or indoor environment. Besides, some outdoor experiments in an uncontrollable turbulent environment are limited to the pre-planned path or using the discrete action space-based maneuver [31–34].

1.4 Outline of the Thesis

The rest of the thesis is organized as follows. In Section II describes overview of the thesis. It contains preliminaries to better understand of the thesis and problems what this thesis is aimed to solve. In Section III, the strategy of GMM-Infotaxis is explained. Section IV proposes RRT-Infotaxis which is designed for the enviornment with obstacles. The numerical simulations of both algorithms and outdoor experiments for GMM-Infotaxis are explained in section V. Conclusion and future work are given in Section VI.

II Problem overviews and preliminaries

In a two-dimensional search area, an unknown source is located at $\mathbf{r}_0 = [x_0, y_0]^T$ and emits particles with a constant emission rate Q_0 in a turbulent flow. In this paper, the source term includes the location of the source and its release rate, defined as $\mathbf{x} = [Q_0, \mathbf{r}_0]^T$ as the main factor of the source. Other parameters such as the wind speed V, wind direction ϕ, diffusivity D, and the substance lifetime of the source τ are assumed to be known. Note, however, that these can also be estimated as done in [34], and we indeed include D and τ in the source term for outdoor flight experiments.

2.1 Dispersion model

Isotropic plume model

The gas dispersion model is adopted from [7] since this model runs very fast and is suitable for a turbulent condition. Suppose particles are propagated with the isotropic diffusivity D and the substance lifetime of τ. The particles are advected by a mean current or wind speed V where ϕ indicates the wind direction. When the wind blows in the direction of the negative y-axis, ϕ is 0. A mobile agent located at $\mathbf{r}_k = [r_{x,k}, r_{y,k}]^T$ at time step k collects measurements and the actual source is located at $\mathbf{r}_0 = [x_0, y_0]^T$. The dispersion model utilized in this study is the expected concentration at $\mathbf{r}_k$ denoted by $R(\mathbf{r}_k|\mathbf{r}_0)$, as expressed in the form of

$$R(\mathbf{r}_k|\mathbf{r}_0) = \frac{Q_0}{4\pi D|\mathbf{r}_k - \mathbf{r}_0|} \exp \frac{(r_{x,k} - x_0)V \sin\phi}{2D} \exp \frac{-(r_{x,y} - y_0)V \cos\phi}{2D} \exp \frac{-|\mathbf{r}_k - \mathbf{r}_o|}{\lambda} \tag{1}$$

where

$$\lambda = \sqrt{\frac{D\tau}{1 + \frac{V^2\tau}{4D}}}. \tag{2}$$

Gaussian plume model

The Gaussian dispersion model [34, 35] assumes the spread of the gas from the source in the crosswind, horizontal and vertical directions. In this model, the source is released continuously at the gas source origin $\mathbf{r}_0 = [x_0, y_0, z_0]^T \in \mathbb{R}^{3+}$ with release rate of $Q_0 \in \mathbb{R}^+$ and the mean gas concentration at the sensing location $\mathbf{r}_k = [r_{x,k}, r_{y,k}, r_{z,k}]^T \in \mathbb{R}^{3+}$ at time step k is formulated as

$$R(\mathbf{r}_k|\mathbf{r}_0) = \frac{Q_0}{2\pi V \sigma_y \sigma_z} \exp \frac{-{c_k}^2}{2{\sigma_y}^2} \Big(\exp \frac{-(r_{z,k} - z_0)^2}{2{\sigma_z}^2} + \exp \frac{-(r_{z,k} + z_0)^2}{2{\sigma_z}^2} \Big), \tag{3}$$

where c_k is the crosswind distance from the source with mean wind velocity V. The standard deviations of concentration σ_y and σ_z in the crosswind and vertical direction respectively are defined as

$$\sigma_y = \zeta_1 d_k / \sqrt{1 + 0.0001 d_k} \text{ and } \sigma_z = \zeta_2 d_k / \sqrt{1 + 0.0001 d_k} \tag{4}$$

where d_k is the downwind distance from the source, and ζ_1, ζ_2 are the stochastic diffusion terms in the horizontal and vertical directions respectively. In this thesis, we assumed the mobile agent

flights the same level above the ground and the gas stacks at the same height. Thus, the height of the mobile agent $r_{z,k}$ and stacking height z_0 is known. Therefore, from the following sections, as we only consider 2-dimensional environment, the location of the mobile agent at time step k is defined as $\mathbf{r}_k = [r_{x,k}, r_{y,k}]^T \in \mathbb{R}^{2+}$.

2.2 Sensor model

Particle encountered sensor model

The stochastic process of particle encounters with a sensor is modeled by a Poisson's distribution. The sensor located at $\mathbf{r}_k$ encounters $z \in \mathbb{Z}^+$ particles during a time interval t_0. Then, the sensor measurement is modeled using the number of mean particle encounters during the time interval, $\mu = R(\mathbf{r}_k|\mathbf{r}_0)t_0$, as:

$$p(z|\mu) = \frac{\mu^z}{z!}e^{-\mu}. \tag{5}$$

Note that, in this model, we assume that the gas already reached a steady state, so sensor measurements only change with respect to the sensor location.

Gaussian sensor model

As the actual gas concentration follows stochastic process, the Gaussian sensor model is modeled by Gaussian distribution. The Gaussian sensor model with the Gaussian noise standard deviation $\sigma_g = \sigma_s + \sigma_{env}$ is formulated as:

$$p(z|\mathbf{x}) = \mathcal{N}(z|R(\mathbf{r}_k|\mathbf{r}_0), {\sigma_t}^2) = \frac{1}{\sigma_t\sqrt{2\pi}} \exp -\frac{(z - R(\mathbf{r}_k|\mathbf{r}_0))^2}{2\sigma_t^2}. \tag{6}$$

Among the noise terms, σ_s is proportional to $R(\mathbf{r}_k|\mathbf{r}_0)$ and σ_{env} represents the sensing noise caused by sensing environment such as wind and temperature. Thus, the Gaussian noise standard deviation is expressed as:

$$\sigma_g = \sigma_s + \sigma_{env} = \alpha R(\mathbf{r}_k|\mathbf{r}_0) + \sigma_{env}. \tag{7}$$

Discretized Gaussian sensor model

To compute the utility function of the information-theoretic approach, it is very difficult to use measurements directly in a continuous domain as the equation contains integral and the probability density function is non-linear and non-Gaussian; In utility function which is based on Bayesian framework, prior PDF $p(z_k|\mathbf{x}_k)$ appears where z_k indicates the measurements in a continuous domain and $\mathbf{x}_k$ is the source term parameter at time step k. Thus, continuous sensing ques are needed to be discretized. Let the discretization interval define as $\delta\hat{d}$ and the discretized future measurement set as:

$$\hat{\mathbf{d}}_{k+1} = [\hat{d}_{k+1}^{(min)}, \hat{d}_{k+1}^{(min)} + \delta\hat{d}_{k+1}, ..., \hat{d}_{k+1}^{(max)}] = [\hat{d}_{k+1}^{(1)}, \hat{d}_{k+1}^{(2)}, ..., \hat{d}_{k+1}^{(d_{max})}] \tag{8}$$

where d_{max} represents possible number of measurements at time step (k+1). Note that, the minimum and maximum value in future measurement set is defined by following empirical three-sigma rule; $\mu_{k+1} \pm 3 \cdot \sigma_{g,k+1}$ where $\mu_{k+1}=\sum_{i=1}^{d_{max}} R(\mathbf{r}_k|\mathbf{x}_k^i) \cdot w_k^i$ indicates the expected mean concentration derived by Eq. (6) and $\sigma_{g,k+1} = \alpha \cdot \mu_{k+1} + \sigma_{env}$.

The the measurement probability distribution with the discretized measurement set of Gaussian sensor model can be formulated with cumulative distribution function (CDF) of the standard normal distribution, $\Phi(\cdot)$ [36]. Therefore, the probability $p(\hat{d}_{k+1}^j|\mathbf{x}_k)$ with the associated particle filter weight, w_k^i is represented as:

$$p(\hat{d}_{k+1}^j|\mathbf{x}s_k) = \sum_{i=1}^{N} \left[\Phi\left(\frac{\Delta\hat{d}_{k+1}^j + \delta\hat{d}}{\hat{\sigma}_{g,k+1}^i} \right) - \Phi\left(\frac{\Delta\hat{d}_{k+1}^j}{\hat{\sigma}_{g,k+1}^i} \right) \right] w_k^i \tag{9}$$

where

$$\begin{aligned} \Delta\hat{d}_{k+1}^j &= \hat{d}_{k+1}^j - R(\mathbf{r}_{k+1}|\mathbf{x}_k^i), \\ \sigma_{g,k+1}^i &= \alpha R(\mathbf{r}_{k+1}|\mathbf{x}_k^i) + \sigma_{env}. \end{aligned} \tag{10}$$

Binary sensor model

As the proposed approach which will be explained in the following sections have to compute receding horizon steps m, binary sensor model is introduced to release the computational load. It has only two sensor measurement values, 1 (when detected) and 0 (not detected) denoted as the future binary measurement as $\hat{b} \in [0, 1]$. The probability of the measurement at time step $(k + n)$ considering m steps ($n \leq m$) is represented as:

$$p(\hat{b}_{k+n}|\mathbf{x}_k) = \begin{cases} \beta & \text{if } \hat{b}_{k+n} = 0 \\ 1 - \beta & \text{if } \hat{b}_{k+n} = 1. \end{cases} \tag{11}$$

The probability, β, can be formulated as done in Eq. (9). Thus, it is expressed as:

$$\beta = \sum_{i=1}^{N} \left[\Phi\left(\frac{\Delta\bar{c}_{k+n}^{(i)}}{\sigma_{g,k+n}^{(i)}} \right) w_k^{(i)} \right] \tag{12}$$

where

$$\begin{aligned} \Delta\bar{c}_{k+n}^{(i)} &= \bar{c}_k - R(\mathbf{r}_{k+n}|\hat{\mathbf{x}}_k^{(i)}), \\ \sigma_{g,k+n}^{(i)} &= \alpha R(\mathbf{r}_{k+1}|\hat{\mathbf{x}}_k^{(i)}) + \sigma_{env}. \end{aligned} \tag{13}$$

For updating the probability of the future measurement, we utilize the current weight of the particle filter at time step k. Sequentially predicting the weights and using them to predict the next after step requires significant computational load. Furthermore, as updating weights, the reliability of the prediction decreases.

To efficiently update the threshold $\bar{c}_k$, it is designed to be changed adaptively with respect to the current sensor measurement:

$$\bar{c}_k = \begin{cases} a\bar{c}_{k-1} + (1-a)\bar{c}_{k-1} & \text{if } k > 1, c_k > \bar{c}_{k-1} \\ \bar{c}_{k-1} & \text{if } k > 1, c_k \leq \bar{c}_{k-1} \\ c_k & \text{if } k = 1. \end{cases} \tag{14}$$

where a is 0.5 in this thesis. The threshold monotonically increases only when the new measurement is greater than the current threshold so that the mobile agent gradually moves towards to get higher concentration. Updating threshold can facilitate exploitation as the mobile agent collects measurements.

2.3 Information-theoretic searching strategy

The idea of information-theoretic search, called 'Infotaxis', was first proposed by Vergassola et al. [7]. Infotaxis is a Bayesian inference method consisting of source term estimation and source search strategy. In Infotaxis, the information gain which is called the Infotaxis reward is computed for all possible next sampling positions based on cardinal movement directions (in general, up, down, left, and right), and the position with the highest reward is selected as the next sampling position. However, using this discrete movement action space might miss a chance to obtain the optimal sampling position.

Source term estimation

The source term, which we want to estimate, includes the location of the source $\mathbf{r}$ and its release rate Q, defined as $\mathbf{x} = [\mathbf{r}, Q]^T$ as the main factor of the hazardous gas dispersion situation. Other parameters such as the wind speed V, wind direction ϕ, diffusivity D, and the substance lifetime of the source τ are assumed to be known; these parameters can be identified by using the meteorological data and the gas properties. Note that all parameters can be estimated as state variables like as done in [34]. However, in this paper, we simplified the estimation problem by using external information (i.e. meteorological data and the gas properties) to focus more on the source search strategy rather than the estimation itself.

In this paper, we utilize Bayesian framework for estimating the source term. Based on the Bayesian inference, the current estimated source term at time step k is represented by a posterior probability density function (PDF) as:

$$p(\mathbf{x}_k|z_{1:k}) = \frac{p(z_k|\mathbf{x}_k)p(\mathbf{x}_k|z_{1:k-1})}{p(z_k|z_{1:k-1})} \tag{15}$$

where

$$p(z_k|z_{1:k-1}) = \int p(z_k|\mathbf{x}_k)p(\mathbf{x}_k|z_{1:k-1})d\mathbf{x}_k. \tag{16}$$

The prior PDF of the source term, $p(\mathbf{x}_k|z_{1:k-1})$, the likelihood, $p(z_k|\mathbf{x}_k)$ which could be obtained by using Eqs. (1) and (3), and the marginal likelihood, $p(z_k|z_{1:k-1})$, are necessary to estimate

the posterior PDF. The measurements collected until the current time step is represented by $z_{1:k} = \{z_1(\mathbf{r}_1), z_2(\mathbf{r}_2), \cdots, z_k(\mathbf{r}_k)\}$.

Computing the analytical solution of $p(\mathbf{x}_k|z_{1:k})$ is impossible since the source term has highly non-linear and non-Gaussian property. Thus, we use the Sequential Monte Carlo methods (i.e. particle filter) [25] to estimate the source term. The particle filter has an advantage when it comes to solving non-linear and non-Gaussian problems. The approximated posterior PDF using the particle filter is expressed as

$$p(\mathbf{x}_k|z_{1:k}) \approx \sum_{i=1}^{N} w_k^i \delta(\mathbf{x} - \mathbf{x}_k^i), \tag{17}$$

where $\mathbf{x}_k^i$ is i-th sampled particle from the particle filter which has the corresponding weight w_k^i at time step k, and N sampled particles represent the posterior PDF of source term by a Dirac delta function, $\delta(\cdot)$. The particle filter sequentially updates weights at each iteration by Eq (15). We assume the gas source is stationary, so $\mathbf{x}_k^i = \mathbf{x}_{k-1}^i$ and the prior distribution at k time step is the same as the posterior distribution of the source term at time step $k-1$ which is represented by $\mathbf{x}_{k-1}^i$ and corresponding weights. Additionally, as the marginal likelihood, $p(z_k|z_{1:k-1})$, does not depend on the source term state, it is treated as a constant to update the weight. Then, the unnormalized posterior weight of i-th particle is updated by:

$$\bar{w}_k^i = p(z_k|\mathbf{x}_{k-1}^i) \cdot w_{k-1}^i \tag{18}$$

The normalized weight is given as:

$$w_k^i = \frac{\bar{w}_k^i}{\sum_{j=1}^{N} \bar{w}_k^j}. \tag{19}$$

To prevent the degeneracy problem, we used the resampling method [37]. The particles are resampled when the effective number of the particle filter, $N_{eff} \approx \frac{1}{\sum_{i=1}^{N}(w_k^i)^2}$, falls below a certain value [38]. However, as the sampling from the unknown target distribution is difficult, we use important sampling (IS); IS generates particles from the known distribution (called the importance or proposal distribution) which can approximate the posterior distribution. The importance distribution for drawing particle samples utilizes the estimated source term distribution at the previous time step similar to previous studies [8–10]. The Markov chain Monte Carlo (MCMC) method is also utilized to increase the diversity of sampled particles [37].

Infotaxis

Infotaxis is a strategy which locally maximizes the expected information gain [7]. In other words, it maximizes the reduction in the entropy (i.e. uncertainty) of the potential source term PDF. The agent chooses the best maneuver $\mathbf{u}_k^*$ from an admissible set of actions in a discrete domain, $\mathbb{U}_I = \{\uparrow, \downarrow, \leftarrow, \rightarrow\}$, as:

$$\mathbf{u}_k^* = arg \max_{\mathbf{u}_k \in \mathbb{U}_I} I(\mathbf{u}_k) \tag{20}$$

where the expected information gain $I(\mathbf{u}_k)$ is defined as the following utility function.

$$I(\mathbf{u}_k) = p(\mathbf{r}_{k+1})H_k - (1 - p(\mathbf{r}_{k+1}))(E[\hat{H}_{k+1}(\hat{z}_{k+1})] - H_k) \tag{21}$$

where

$$H_k = -\int p(\mathbf{x}|z_{1:k}) \log p(\mathbf{x}|z_{1:k}) d\mathbf{x} \tag{22}$$

is the Shannon's entropy. The first term in Eq. (21) works locally and only valid when the source origin is exactly located at $\mathbf{r}_{k+1}$ where the expected source location needs to be one of the grid points of the environment [8]. According to the Eq. (18), the weight of the particle filter can represent the posterior PDF, $p(\mathbf{x}|z_{1:k})$. The entropy can then be computed approximately using the normalized weight in Eq. (19) as

$$H_k = -\sum_{i=1}^{N} w_k^i \log w_k^i \tag{23}$$

The expectation operator E in Eq. (21) is a function of the expected measurement $\hat{z}_{k+1}$ at the next sampling position $\mathbf{r}_{k+1} = \mathbf{r}_k + \mathbf{u}_k$. The expected entropy at time step (k+1) is written as

$$E[\hat{H}_{k+1}] = \sum_{\hat{z}_{k+1}=0}^{z^{max}} p(\hat{z}_{k+1}|\mathbf{x}_k) \hat{H}_{k+1}(\hat{z}_{k+1}) \tag{24}$$

where

$$\hat{H}_{k+1}(\hat{z}_{k+1}) = -\int p(\hat{\mathbf{x}}_{k+1}|z_{1:k}, \hat{z}_{k+1}) \log p(\hat{\mathbf{x}}_{k+1}|z_{1:k}, \hat{z}_{k+1}) d\hat{\mathbf{x}}_{k+1}. \tag{25}$$

Here, the maximum number of particle encountered is denoted as z^{max}. Similarly, as done in Eq. (18), the weight of the potential source term is updated as:

$$\hat{\hat{w}}_{k+1}^i = p(\hat{z}_{k+1}|\mathbf{x}_k^i) \cdot w_k^i. \tag{26}$$

Hence, the expectation of the entropy at time step (k+1) can be expressed as:

$$E[\hat{H}_{k+1}] = -\sum_{\hat{z}_{k+1}=0}^{z^{max}} \Big(p(\hat{z}_{k+1}|\mathbf{x}_k) \sum_{i=1}^{N} (\hat{w}_{k+1}^i) \log (\hat{w}_{k+1}^i) \Big), \tag{27}$$

where $\hat{w}_{k+1}^i$ is the normalized weight related to the set of possible measurements at the next position, $\mathbf{r}_{k+1}$. Finally, the the utility function Eq. (21) can be approximated by

$$\begin{aligned} I(\mathbf{u}_k) \approx & -p(\mathbf{r}_{k+1}) \sum_{i=1}^{N} w_k^i \log w_k^i \\ & - (1 - p(\mathbf{r}_{k+1})) \Bigg(\sum_{\hat{z}_{k+1}=0}^{z^{max}} \Big(p(\hat{z}_{k+1}|\mathbf{x}_k) \sum_{i=1}^{N} (\hat{w}_{k+1}^i) \log (\hat{w}_{k+1}^i) \Big) - \sum_{i=1}^{N} w_k^i \log w_k^i \Bigg). \end{aligned} \tag{28}$$

The first term of the right hand side in Eq. (21) is only valid when the expected source origin coincides with the real source origin. Furthermore, as we consider the admissible actions in a continuous domain, computing the probability $p(\mathbf{r}_{k+1})$ requires much significant computational

load. Because of these reasons, as done in [8], the first term in Eq. (21) is ignored and only the second term is utilized. Then, the final utility function is given by

$$I(\mathbf{u}_k) = \sum_{\hat{z}_{k+1}=0}^{z^{max}} p(\hat{z}_{k+1}; \mathbf{x}_k)\Big(\sum_{i=1}^{N} \hat{w}_{k+1}^i \log \hat{w}_{k+1}^i\Big) - \sum_{i=1}^{N} w_k^i \log w_k^i. \tag{29}$$

III Source Search Strategy 1: GMM-Infotaxis

3.1 Gaussian Mixture Model-Based Infotaxis

The admissible set of actions in the Infotaxis approach is based on the grid-based method, i.e., $\mathbb{U}_I = \{\uparrow, \downarrow, \leftarrow, \rightarrow\}$, so the maneuver of the agent is limited. The limited maneuver allows the mobile agent to obtain measurements at corresponding grid points only and may miss a chance to get useful and informative measurements from the optimal sampling positions. Furthermore, the second term of the Infotaxis reward is known to be biased toward exploration rather than exploitation, [26]. To address these problems, the Gaussian mixture model (GMM) is introduced to generate a certain number (denoted as L) of new action candidates in a continuous domain, $\mathbb{U}_G = \{\mathbf{u}_1^G, \mathbf{u}_2^G, ..., \mathbf{u}_L^G\}$, by utilizing potential source locations. This method is more likely to guide the mobile agent toward the source origin so that it enables more efficient exploitation. From the following, we briefly introduce the GMM and how to use it with the particle filter to generate action candidates.

Gaussian Mixture Model (GMM)

The GMM is a function which is composed of several Gaussian distributions with three components: mean, covariance and mixing probability [**?**]. Let us denote the number of models of the GMM as L, and its associated sets of mean, covariance, and mixing coefficient as $\mathbf{M} = \{m_1, m_2, ..., m_L\}$, $\Sigma = \{\Sigma_1, \Sigma_2, ..., \Sigma_L\}$, and $\Pi = \{\pi_1, \pi_2, ..., \pi_L\}$, respectively. Besides, the elements of Π satisfy the constraints that $\sum_{i=1}^{L} \pi_i = 1$. Depending on L, data sets are clustered by the Gaussian distribution as illustrated in Fig. 2. The GMM with Gaussian distributions is expressed as:

$$p(\mathbf{y}|\mathbf{M}, \Sigma, \Pi) = \sum_{i=1}^{L} \pi_i G(\mathbf{y}|m_i, \Sigma_i), \tag{30}$$

where $\mathbf{y}$ is a n-dimensional data vector, i.e., measurements, and $G(\mathbf{y}|m_i, \Sigma_i)$ is the Gaussian distribution. The form of the n-variate Gaussian distribution is represented as:

$$\begin{aligned} G(\mathbf{y}|m_i, \Sigma_i) = & \frac{1}{(2\pi)^{n/2}\sqrt{|\Sigma_i|}} \\ & \cdot \exp\Big(-\frac{1}{2}(\mathbf{y} - m_i)^T \Sigma_i^{-1} (\mathbf{y} - m_i)\Big). \end{aligned} \tag{31}$$

In this study, the data for clustering is the possible source locations on x and y axis, computed by particles from the particle filter. Thus, the Gaussian distributions are formed in a two-dimensional space with potential source locations, that is, $\mathbf{y}$ in Eq. (20) is replaced with $\mathbf{r}_k$.

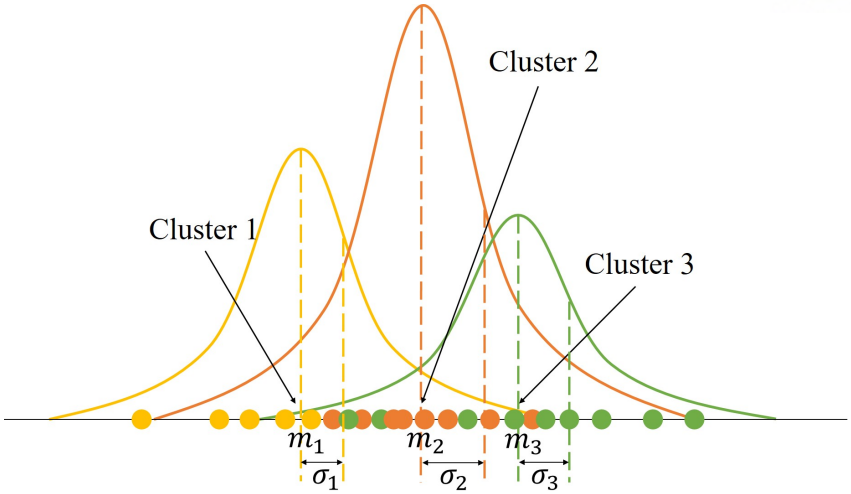

(a) 1-D Gaussian mixture model

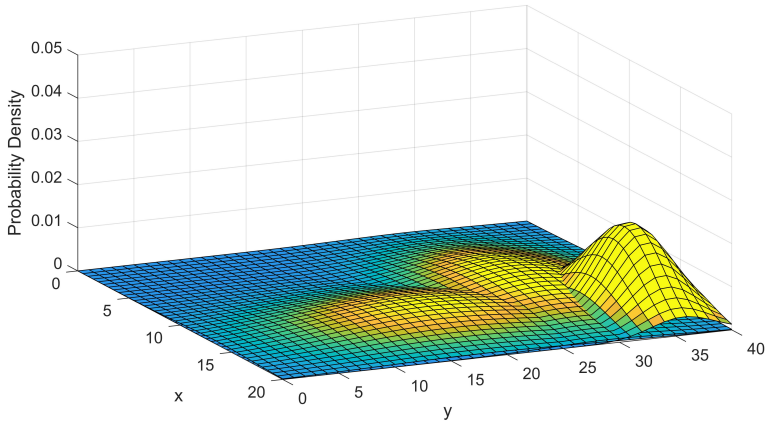

(b) 2-D Gaussian mixture model

Figure 2: 1-D and 2-D Gaussian mixture models.

To optimize the parameters of the GMM, the maximum likelihood estimation is used, which is the most popular and well-established method via the expectation-maximization algorithm as in [39].

3.2 Search process of GMM-Infotaxis

As the high-density region of particles from the particle filter is likely to be the potential source location, clustered particles by the clustering algorithm represent the potential regions that might contain the source. To utilize this property, this study uses the GMM among other clustering algorithms [40] as it can produce the Gaussian distributions with the useful information: the mean and variance of the clusters. The mean values of the clustered data $\mathbf{M}$ are used as the directions of the action candidate set. This GMM-action candidate set is generated a certain distance (i.e., size of d) away from the current agent location towards the direction of the mean of the GMM as illustrated in Fig. 3. We assumed that the number of Gaussian distributions L is 3,

so the direction of the GMM-action set is indicated as m_1, m_2, and m_3. Along with the clustered points, we put a certain number of random points into the GMM-action set additionally to avoid local optima (e.g., when the particles are grouped in the wrong area where the source does not exist). Thus, the GMM-action set consists of the actions which are directed to $\mathbf{M}$ and d distance from the agent and random points defined as $\mathbb{U}_G = \{\mathbf{u}_1^G, \mathbf{u}_2^G, ..., \mathbf{u}_L^G\}$.

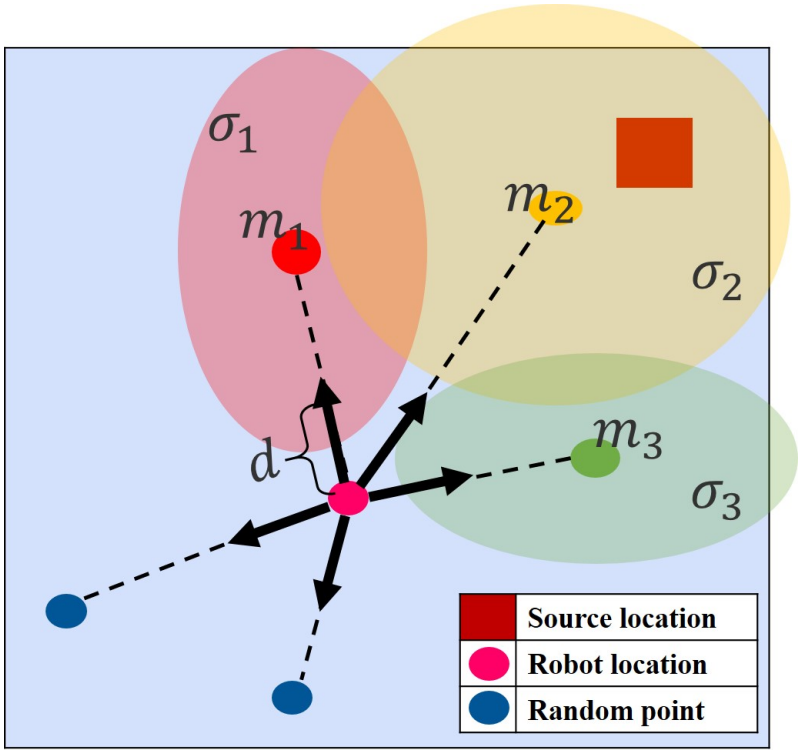

Figure 3: The GMM-action set.

To benefit from the GMM-action set, particles from the particle filter need to have sufficiently accurate information for the source location. In other words, the particles should be converged to a certain level; otherwise, the GMM-action set would not provide any useful information about the source, particularly during the initial stage of the particle filter. To address this issue, we introduce the switching process with selects action candidates between the Infotaxis-action set $\mathbb{U}_I = \{\uparrow, \downarrow, \leftarrow, \rightarrow\}$ and the GMM-action set $\mathbb{U}_G = \{\mathbf{u}_1^G, \mathbf{u}_2^G, ..., \mathbf{u}_L^G\}$ depending on the standard deviation (or variance) of the GMM. As the standard deviation indicates the convergence of the particle filter which implies the reliability of the estimated source term, it is used as the metric for switching the action sets.

To this end, the standard deviations of GMM clusters are first computed from the covariance Σ in Eq. (19). As clustering is conducted in a two-dimensional space, Σ is 2 by 2 matrix and the diagonal terms of Σ indicate the variances along x and y axis. Thus, the standard deviation set $\sigma = \{\sigma_1, \sigma_2, ..., \sigma_L\}$ can be computed by the square root of the sum of the diagonal terms from Σ. It is worthwhile noting that the diagonal term of each element in Σ represents the spread of particles. We then set the switching threshold σ_s which decides whether the mobile agent

takes $\mathbb{U}_I$ or $\mathbb{U}_G$. Among the standard deviation set σ, the minimum value is chosen to compare with σ_s. This strategy would encourage exploitation (i.e. switching to the GMM-action set) if there is a cluster with converged particles, which indicates the probable source origin location. In other words, if $\min(\sigma)$ is less than threshold σ_s, the action set is chosen as $\mathbb{U}_G$; otherwise $\mathbb{U}_I$ is used.

Among actions in the selected action set, the best rewarded action will be chosen as the next position computed by Eq. (29). This strategy facilitates the autonomous trade-off between exploration and exploitation. The search and estimation process is terminated when the standard deviation of all the particles of the particle filter, denoted as σ_p, is less than a certain value, σ_t. The overall implementation process of the proposed method is described in Algorithm 1.

3.3 Algorithm Overview

Algorithm 1 GMM-Infotaxis

for $k = 1, 2, \ldots, k_{max}$ **do**
  $z_k \leftarrow$ Read a new sensor measurement
  $\{(\mathbf{x}_{k-1}, w_{k-1}) \rightarrow (\mathbf{x}_k, w_k)\}$ using Eq. (19)
  $\mathbf{M} = \{m_1, m_2, ..., m_L\}$, $\Sigma = \{\Sigma_1, \Sigma_2, ..., \Sigma_L\}$ using Eq. (30)
  $\sigma = \{\sigma_1, \sigma_2, ..., \sigma_L\}$ from Σ
  if $\min(\sigma) < \sigma_s$ **then**
    $\mathbb{U} = \mathbb{U}_G \leftarrow$ Select GMM-action set
  else
    $\mathbb{U} = \mathbb{U}_I \leftarrow$ Select Infotaxis-action set
  end if
  $I(\mathbf{u}_k)$ computation with Eq. (29)
  $\mathbf{u}_k^* = arg\max_{\mathbf{u}_k \in \mathbb{U}} I(\mathbf{u}_k) \leftarrow$ Next best maneuver
  if $\sigma_p < \sigma_t$ **then**
    break;
  end if
  $\mathbf{r}_{k+1} = [r_{x,(k+1)}, r_{x,(y+1)}]^\top = [r_{x,k}, r_{x,k}]^\top + \mathbf{u}_k^* \leftarrow$ next sampling position $\mathbf{r}_{k+1}$
end for

IV Source Search Strategy 2: RRT-Infotaxis

In real life, source searche is performed in complex environments such as urban areas full of obstacles rather than open spaces. Local optima often occurs under these conditions. For instance, the mobile agent moves around explored area or visits the same location multiple times. To solve this problem, predicting long-term states is needed. To this end, Rapidly-exploring random trees (RRT) which is the sampling based path planning algorithm combined with the Infotaxis is introduced. The advantage of introducing RRT is not only obstacle avoidance but also preventing the mobile agent from falling into local optima by considering multiple steps ahead. Firstly, as RRT distributes random samples in obstacle-free continuous domain, the action candidates of the mobile agent generates path avoiding obstacle. Secondly, by utilizing the sampled path, predicting several steps ahead (i.e., receding horizon method) is able to solve local optima. In conventional cognitive search [8], the source search is based on maximizing entropy reduction during decision making so that the mobile agent moves towards more likely to reduce uncertainty. However, for efficient source search, balancing exploration and exploitation is essential. Thus, a new utility function is proposed, which consists of maximizing entropy reduction and minimizing the path length for the search. By adopting the receding horizon approach with a new utility function, RRT-Infotaxis outperforms GMM-Infotaxis and conventional Infotaxis. From the following, the principle of RRT is briefly explained. After that, the proposed utility function is described. Lastly, the overall process of RRT-Infotaxis is given.

4.1 Rapidly-exploring Random Trees (RRT)

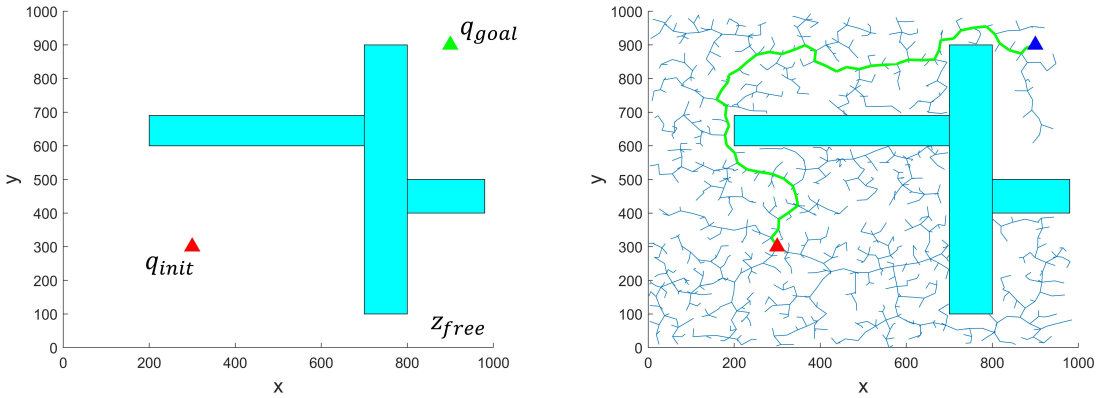

(a) Initial state (b) Terminated state

Figure 4: The run for RRT.

Rapidly-exploring Random Trees (RRT) is a sampling based path planning algorithm suggested by Steven M. LaValle and James J. Kuffner Jr [41]. It is designed to search efficiently non-convex and high-dimensional spaces. By randomly generating samples in a continuous space, it inherently fills the space biased to unexplored areas evenly. Let the given space be denoted

by a set $\mathbb{Z} \subset \mathbb{R}^2$ as we consider 2-dimensional configuration space. The area occupied with obstacles is represented by $\mathbb{Z}_{obs}$ and obstacle free area as $\mathbb{Z}_{free}$. RRT constructs tree by sampling random nodes in $\mathbb{Z}_{free}$. From the starting point q_{init}, the tree gradually expands and the process ends when the tree expands sufficiently near the goal point, q_{goal}. During each iteration of the algorithm, random sample q_{rand} is sampled in Z and if it lies in Z_{free}, the closest sample $q_{nearest}$ in the tree T from q_{rand} is selected. If q_{rand} is accessible to $q_{nearest}$ and distance between them is less than the predefined movement distance Δ, $q_{nearest}$ is considered as the new node q_{new} and added to the tree T. However, if the distance is longer than Δ, new sample towards from $q_{nearest}$ to the q_{rand} at the distance Δ is considered as q_{new}. Figure. 4 shows when the RRT algorithm declares path reached goal point from the initial state by sampling random samples in obstacle free-area. The process of tree expand is described in Fig. 5.

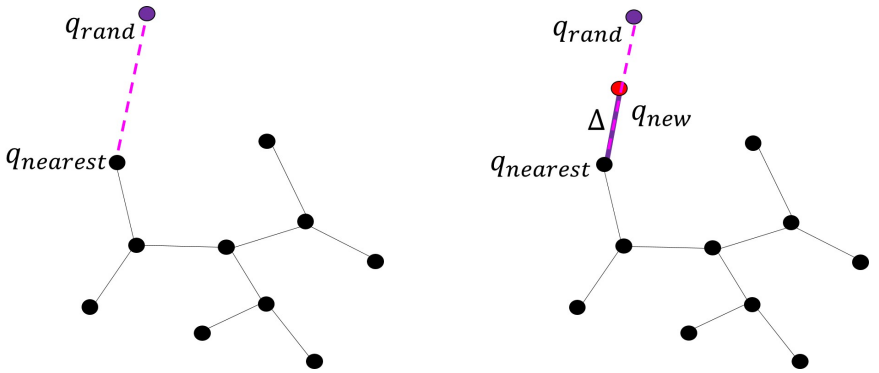

(a) Generate random sample q_{rand} (b) Add new node q_{new} to the tree T

Figure 5: Tree expansion of the RRT.

The representative characteristics of RRT can be categorized twofold. First, it generates path avoiding obstacles. Second, it makes random samples in a continuous domain with simple implementation so that the tree tends to expand towards unexplored area. By adopting these properties, suggested strategy is able to choose efficient action candidates of mobile agent.

4.2 Utility function of RRT-Infotaxis

The conventional utility function of information-theoretic strategy utilizes the entropy (i.e., uncertainty) [8]. As mentioned earlier, this method is known to be biased to exploration rather than exploration, [26]. Thus, by introducing a new utility function, proposed RRT-Infotaxis facilitates proper exploration and exploitation in obstacle-rich environments. Combined with information-theoretic utility function and the cost function of RRT, derived from the A* algorithm [42], the mobile agent balances exploration (i.e., looking for the source ques) and exploitation (i.e., move towards the source origin). The suggested new utility function is comprised of two parts: maximizing entropy reduction and minimizing search path.

Maximizing entropy reduction

To maximize entropy reduction, the Infotaxis utility function, Eq. (29) explained in the previous section, is adopted. Among all the branches of RRT tree, T, generated by N_{tn} number of nodes described in Fig. 6 (a), let k^{th} branch of the tree has n nodes. The branch can be formulated by a set $\mathbf{V}_k = \{\mathbf{v}_{k,1}, \mathbf{v}_{k,2}, ..., \mathbf{v}_{k,n}\}$ as shown in Fig. 6 (b) and each element indicates 2-dimensional location in search area. Here, we consider m receding horizon step. As there are some branches which have longer or less than m number of nodes, only the branches having at least m number of nodes are considered as the action candidate sets as illustrated in Fig. 6 (b). This process is called tree pruning. Remained branches included in pruned trees, T_p are the action candidate sets for the mobile agent. Each branch is considered as the receding horizon path of the mobile agent. Therefore, each node in one branch is the action candidate for the long-term states. To get the entropy reduction considering m receding horizon steps, m number of nodes in each branch has to be considered. To release the computational load, binary sensor model described in Section 2.2 is adopted.

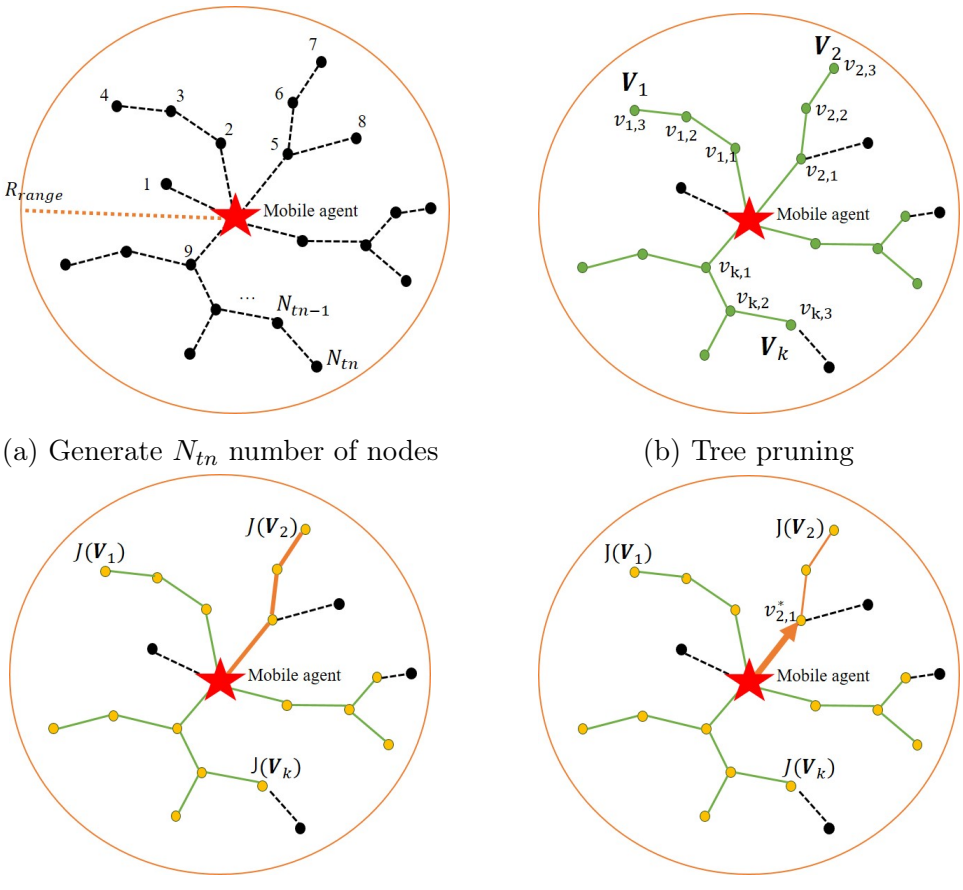

(a) Generate N_{tn} number of nodes (b) Tree pruning

(c) Compute utility function (d) Move toward the best rewarded action

Figure 6: The example process of selecting the next best action of RRT-Infotaxis when m is 3.

Thus, the entropy reduction of each node in one branch using binary sensor is expressed as:

$$I(\mathbf{v}_{k,n}) = -\sum_{i=1}^{N} w_k^i \log w_k^i + \sum_{\hat{b}_{k+n}=0}^{1} p(\hat{b}_{k+n}|\mathbf{x}_k) \cdot \sum_{l=1}^{N} (\hat{w}_{k+n}^l) \log (\hat{w}_{k+n}^l) \tag{32}$$

All the nodes from the first to the m^{th} node in each branch, which are the action candidates for receding horizon approach, are computed by the Eq. (32) and accumulated. However, as the closest node has the most reliable information, weight factor α is applied when accumulating the results. Finally, utility function of maximizing entropy reduction in RRT-Infotaxis is expressed by:

$$J_1(\mathbf{V}_k) = \sum_{n=1}^{m} \alpha^{(n-1)} I(\mathbf{v}_{k,n}). \tag{33}$$

Minimizing search path

To improve the performance with regard to shortening the search path, the cost function of RRT is introduced. Conventional cost function calculates the path length from the initial state to the current state and adds the Euclidean distance between the current point and goal point, which is derived from A* cost function [42]. However, in the case of source search, as the goal is to estimate the source origin, the exact source location is not known. Thus, estimated source origin $\hat{\mathbf{r}}_0$ is considered as the goal point and the goal is updated with every iteration. As the source search process proceeds, the estimated location becomes more accurate. It implies that as the mobile agent collects measurements, the mobile agent tends to move to the correct source location. Finally, the cost function of minimizing search path is formulated by:

$$J_2(\mathbf{V}_k) = \sum_{n=1}^{m} |\mathbf{v}_{k,n} - \mathbf{v}_{k,n-1}| + |\hat{\mathbf{r}}_0 - \mathbf{v}_{k,m}| \tag{34}$$

where $\mathbf{v}_{k,0}$ indicates current location of the mobile agent $\mathbf{r}_k = [x_k, y_k]$. In the above equation, the left term of the right-hand side indicates that the sum of the path lengths from current to the m steps ahead location of the mobile agent and right term refers the Euclidean distance between m step ahead location and the goal point (i.e., estimated source origin $\hat{\mathbf{r}}_0$).

Finally, the proposed utility function for the RRT-Infotaxis is expressed as:

$$J(\mathbf{J}_k) = \epsilon J_1(\mathbf{V}_k) - (1-\epsilon) J_2(\mathbf{V}_k) \tag{35}$$

where ϵ is the weight of the each function. In this thesis, ϵ is chosen as 0.5 to make the two tendency of the function work equally. Note that, as the cost function of the RRT is supposed to minimize the cost, the utility function, $J_2(\mathbf{V}_k)$, has minus sign in the final utility function, $J(\mathbf{V}_k)$. The next best action of RRT-Infotaxis is the one step ahead action in the best rewarded branch $\mathbf{V}_k$ considering m steps. The chosen best maneuver $\mathbf{v}_{k,1}$ is defined as:

$$\mathbf{v}_{k,1}^* = arg \max_{\mathbf{V}_k \in T_p} J(\mathbf{V}_k). \tag{36}$$

As the estimation process proceeds, utility function $\mathbf{J}_1$ would shows the similar value as the mobile agent already gathered enough measurements. Thus, in this situation, the function $\mathbf{J}_2$ would plays a main role to lead the mobile agent. As this function is designed to chose the shortest path to the estimated source location, the mobile agent is highly likely to move to the region around the true source. In this regard, proposed utility function takes reasonable balance between exploration and exploitation.

4.3 Search process of RRT-Infotaxis

The overall process of the RRT-Infotaxis is described in Fig. 6. The tree is generated with N_{tn} number of RRT nodes only in the limited region, R, with a radius of R_{range} as shown in Fig. 6 (a). After that, the tree pruning process is conducted. With this process, only branches containing at least m number of nodes are selected among generated branches in the tree. Each branch is the path candidates of the mobile agent. By computing utility function using Eq. (**??**) and Eq. (36), the best rewarded branch is chosen. Finally, described in Fig. 6 (d), the mobile agent moves one step to the best rewarded branch. With each iteration, the RRT-Infotaxis algorithm repeatedly erases the old tree and creates a new tree by centering the current position of the mobile agent with every time step.

4.4 Algorithm Overview

The estimation process is the same with GMM-Infotaxis. With the particle filter, the source term is estimated by updating its weight. The detail of the functions in Algorithm. 2 is described as follows.

- Sample: This function generates random position q_{rand} which is included in the region R_{range}.
- FindNearestNode: This function results the nearest node from other nodes in T to q_{rand}.
- Steer: This function generates q_{new} along the path from $q_{nearest}$ towards q_{rand} at a distance Δ where Δ is the incremental distance.
- TreePrune: This function returns all of the trees that have at least m which is the RH-step of nodes.

Algorithm 2 RRT-Infotaxis

T.init(q_{init})
for $k = 1, 2, \ldots, k_{max}$ **do**
  $z_k \leftarrow$ Read a new sensor measurement
  $\{(\mathbf{x}_{k-1}, w_{k-1}) \rightarrow (\mathbf{x}_k, w_k)\}$ using Eq. (19)
  $q_{new} \leftarrow q_{init} = [r_{x,k}, r_{y,k}]$
  while $N_{seed} < N_{tn}$ **do**
    $q_{rand} \leftarrow$ Sample(q_{rand})
    $q_{nearest} \leftarrow$ FindNearestNode(q_{rand}, T)
    $q_{new} \leftarrow$ Steer($q_{nearest}, q_{rand}$)
    if Obstacle Free **then**
      T.add_node(q_{new})
      T.add_vertex($q_{new}, q_{nearest}$)
      $N_{seed} = N_{seed} + 1$
    end if
  end while
  $T_p \leftarrow$ TreePrune(T)
  for $\mathbf{v}_{k,k:k+m-1} \in \mathbf{V}_k$ **do**
    for $n = 1, 2, ..., m$ **do**
      $\{(\mathbf{x}_k, w_k) \rightarrow (\hat{\mathbf{x}}_{k+n})\} \leftarrow$ Receding horizon method
    end for
    $[\hat{b}_{k+1}, ..., \hat{b}_{k+m}] \leftarrow$ Collect binary sensor measurements
    $J(\mathbf{J}_k) = \epsilon J_1(\mathbf{V}_k) - (1-\epsilon) J_2(\mathbf{V}_k)$
  end for
  $J(\mathbf{V}_k)$ computation with Eq. (35)
  $\mathbf{v}^*_{k,1} = arg\max_{\mathbf{V}_k \in T_p} J(\mathbf{V}_k) \leftarrow$ Next best maneuver
  Clear T
  if $\sigma_p < \sigma_t$ **then**
    break;
  end if
  $\mathbf{r}_{k+1} = [r_{x,(k+1)}, r_{y,(k+1)}]^\top = [r_{x,k}, r_{y,k}]^\top + \mathbf{v}^*_{k,1} \leftarrow$ next sampling position $\mathbf{r}_{k+1}$
end for

V Results

In this section, the results of the numerical simulations and experiments of GMM-Infotaxis and numerical simulations of RRT-Infotaxis are presented. For the GMM-Infotaxis, the effect of the GMM is explained and the process of finding out the optimal parameters such as the number of models for the GMM-Infotaxis is described. After that, with defined parameters, the effect of wind and source release rate are analyzed. The performance of GMM-Infoatxis compared with Infotaxis is validated with outdoor flight experiment.

For the RRT-Infotaxis, the number of nodes and receding horizon steps affect on the performance of RRT-Infotaxis. To get the proper parameters, numerical simulations are conducted. After that, with the environment with obstacles, the performance of RRT-Infotaxis is compared with that of GMM-Infotaxis and Infotaxis.

5.1 Numerical simulations: GMM-Infotaxis

In order to validate the performance of the proposed GMM-Infotaxis algorithm compared to the Infotaxis approach [8], we performed Monte Carlo simulations in a 2-D environment. Isotropic plume model and particle encountered sensor model are utilized explained in Section II. The number of models for the GMM affects the performance of the overall algorithm. To draw out the proper number of models in the GMM, which is called a cluster in this paper, we conducted numerical simulations changing the number of clusters. After finding the optimal number of models, the effects of other parameters such as wind speed V and source release rates Q_0 are studied. The performance metrics are the mean search time step (MST), its standard deviation, and the success rate (SR). The search process is terminated when the standard deviation of the estimated source location in the particle filter, σ_p, falls below a threshold σ_t. After termination, if the error between the estimated and actual source location is less than a threshold, d_s, the estimation is regarded as a success.

The effect of the GMM

To figure out the optimal number of particle clusters for the GMM (i.e. the number of GMM-action candidates), we compared the mean search time (MST) with the different number of clusters. Besides, to verify the efficiency of switching two action sets, two approaches are compared: only GMM-action set and switching between grid and GMM-action set. The simulation environment setup follows the below parameters and all the parameters are non-dimensional:

- True source term: $Q_0 = 1, \mathbf{r}_0 = [17.5, 32.5]^\top$;
- Initial position of the mobile agent: $\mathbf{r}_1 = [5, 5]^\top$;
- Search area: $A = 20 \times 40$, wind velocity in the negative y direction $V = 5$, diffusivity $D = 1$, and finite lifetime $\tau = 250$;

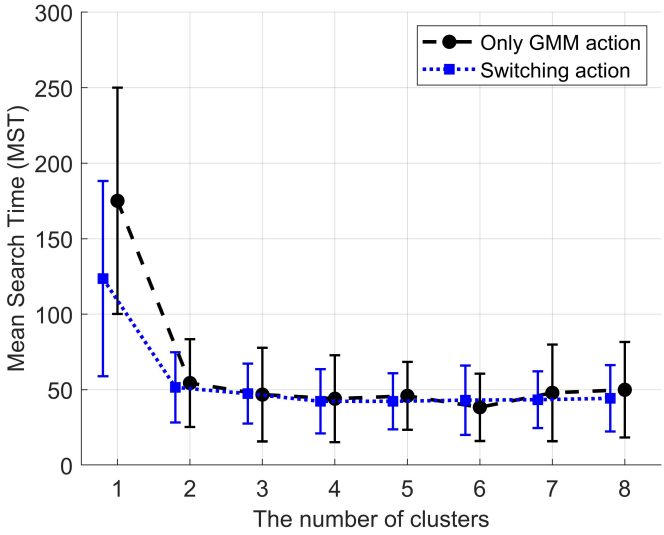

Figure 7: The MST of the algorithms with varying the number of clusters averaged over 100 Monte Carlo simulations for each cluster.

- Movement step size: $d = 5$;
- Number of particles for the particle filter: $N = 3,000$;
- GMM parameters: threshold for the switching action: $\sigma_s = 3\sigma_t$;
- Terminal conditions: standard deviation of the particle filter $\sigma_t = 1.5$, and the estimation success threshold $d_s = 3$.

As the number of clusters increases, the MST of both approaches decreases and converges to about 50 with more than two clusters as shown in Fig. 7. However, the standard deviation is smaller for the case of the switching action compared with the only GMM-action case, showing the benefit of using the proposed switching process. As the number of clusters increases, the computational load soars as well; hence, we choose three clusters with switching between grid and GMM-action sets according to the switching criteria from the following simulations.

We also compare the MST of the GMM-Infotaxis approach with three different grid-based action sets including Infotaxis (4), (8), and (12), in order to show the efficiency of the proposed approach. Infotaxis (4) has an action set of $\{\rightarrow, \uparrow, \leftarrow, \downarrow\}$; in other words, each action candidate is separated with the 90° interval. The action set of Infotaxis (8) and (12) has eight action candidates with the 45° interval and twelve action candidates with the 30° interval, respectively. As shown in Fig. 8, the proposed GMM-infotaxis using only three *informed* action candidates outperforms Infotaxis (4) and (8). Besides, the performance of the GMM-infotaxis approach is similar to that of Infotaxis (12) but with the much fewer number of action candidates. Note that computational load to compute the utility function in Eq. (18) for a large number (i.e 8 or 12) of action candidates would be much higher than computing three GMM distributions, especially when the number of particles is large.

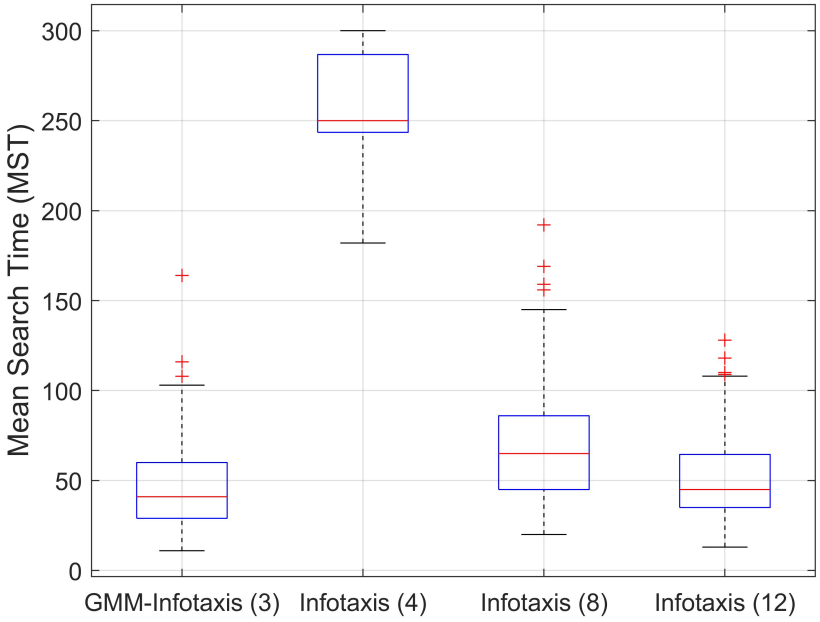

Figure 8: The MST of GMM-Infotaxis and Infotaxis with different admissible action sets.

From the following section, the existing Infotaxis approach [8] and the proposed GMM-Infotaxis are compared. As mentioned above, we choose three clusters for the GMM. We also use two additional random points for the GMM-action candidate set to avoid the local optima where the particles of the particle filter converge to the wrong area. Note that all the parameters for simulations are non-dimensional; however, real flight experiments will have proper dimensions as in Section 5.2.

The effect of source release rate, Q_0

The performance of Infotaxis and GMM-Infotaxis is compared with various source release rates, Q_0, with the fixed wind velocity, $V = 1$.

Q_0	0.2	0.5	1	5	10
Infotaxis					
MST	159.3	112.4	76.1	45.5	44.8
SR	84.5	99.0	100	100	97.0
Localization error	0.7	0.6	0.6	0.7	0.9
GMM-Infotaxis					
MST	151.4	104.3	74.2	41.1	43.1
SR	88.0	100	100	99.5	99.5
Localization error	0.4	0.6	0.6	0.7	0.9

Table 1: Performance comparison with respect to the source release rate Q_0 averaged over 200 Monte Carlo simulations with the movement step size of 1.

Q_0	0.2	0.5	1	5	10
Infotaxis					
MST	164.5	130.8	108.2	62.1	32.7
SR	21.0	41.0	65.5	94.5	95.5
Localization error	0.9	1.1	1.0	1.0	0.9
GMM-Infotaxis					
MST	140.2	79.2	47.0	18.4	14.5
SR	92.0	99.5	99.5	99.5	99.5
Localization error	0.6	0.7	0.8	0.8	0.8

Table 2: Performance comparison with respect to the source release rate Q_0 averaged over 200 Monte Carlo simulations with the movement step size of 5.

As shown in Table 1, with the movement step size d of 1, both algorithms show a similar MST and SR. Where the MST of the GMM-Infotaxis is slightly better than that of the Infotaxis. The estimation error between the true source and estimated source location is denoted as the localization error. When Q_0 is low such as 0.2, the GMM-Infotaxis approach shows the smaller localization error compared with Infotaxis. It is because, as the GMM-Infotaxis generates action candidates in a continuous domain, the mobile agent is able to get better measurements than those of Infotaxis even for the weak source release rate. With a larger movement step size d of 5 as shown in Table 2, GMM-Infotaxis estimates the source term with much lower MST and higher

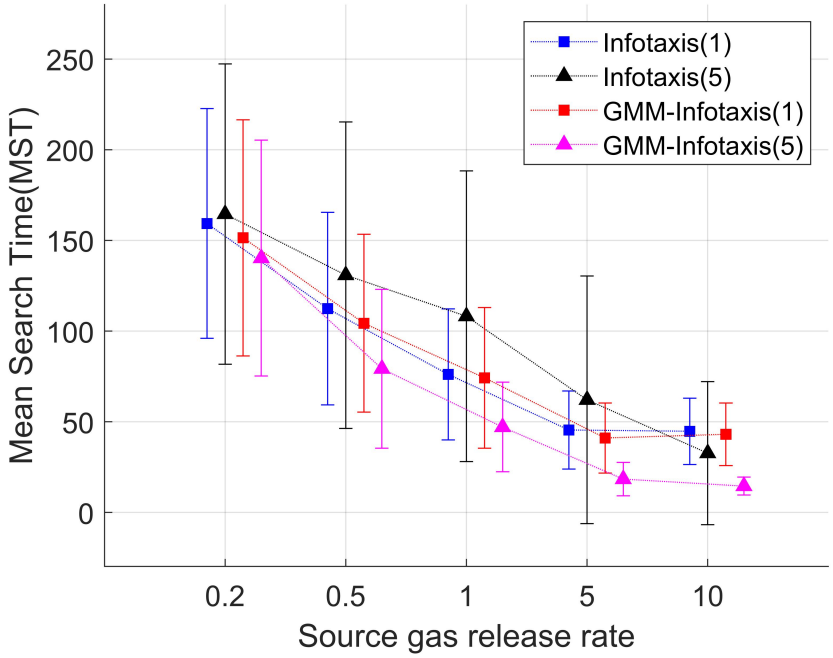

Figure 9: MST with different source release rates and movement step sizes.

SR than those of Infotaxis. For the case of Infotaxis, as the movement step size increases, the possible locations that the mobile agent can get measurements are reduced due to the limitation of the grid-based action candidates. On the other hand, GMM-Infotaxis takes its next action in a continuous domain regardless of the movement step size. This property also affects the localization error. GMM-Infotaxis estimates the location of the source more accurately than Infotaxis as shown in Table 2. The summary of the results is presented in Fig. 9.

The effect of wind velocity, V

The comparison of Infotaxis and GMM-Infotaxis with various wind velocities V and the fixed release rate Q_0 of 1 is shown in Table 3 and 4 and summarized in Fig. 10.

The performance of GMM-Infotaxis is marginally better than that of Infotaxis when the movement step size d is 1 as shown in Table 3. However, when the movement step size becomes 5, GMM-Infotaxis shows a much superior performance to Infotaxis. In all situations, the MST of GMM-Infotaxis is almost less than half of the MST of Infotaxis. Furthermore, in GMM-Infotaxis, the SR is always larger than 90 while the highest SR is only 66.5 for Infotaxis. As illustrated in Fig. **??**, since the agent using Infotaxis can get measurements only at grid points with a fixed resolution, it is hard to obtain more informative measurements, resulting in unnecessary movements around the source origin. On the other hand, GMM-Infotaxis can get various measurements in a continuous domain as shown in Fig. **??**. These results imply that GMM-Infotaxis outperforms the original Infotaxis regardless of the movement step size similar to the previous results with different Q_0. Besides, GMM-Infotaxis is able to estimate the source

V	0.2	0.5	1	5	10
Infotaxis					
MST	85.2	82.1	78.0	73.7	78.0
SR	99.0	100	99.0	99.5	99.0
Localization error	0.6	0.6	0.6	0.5	0.6
GMM-Infotaxis					
MST	85.8	79.0	77.6	64.8	63.7
SR	100	100	100	100	99.0
Localization error	0.6	0.6	0.6	0.5	0.5

Table 3: Performance comparison with respect to the different velocity V averaged over 200 Monte Carlo simulations with the movement step size of 1.

V	0.2	0.5	1	5	10
Infotaxis					
MST	116	112	103	101	114
SR	59.0	66.5	60.5	66.0	55.0
Localization error	1.06	1.06	1.06	1.07	0.99
GMM-Infotaxis					
MST	50	45	45	56	59
SR	99.5	100	97.5	99.5	91.5
Localization error	0.71	0.67	0.68	0.73	0.79

Table 4: Performance comparison with respect to the different velocity V averaged over 200 Monte Carlo simulations with the movement step size of 5.

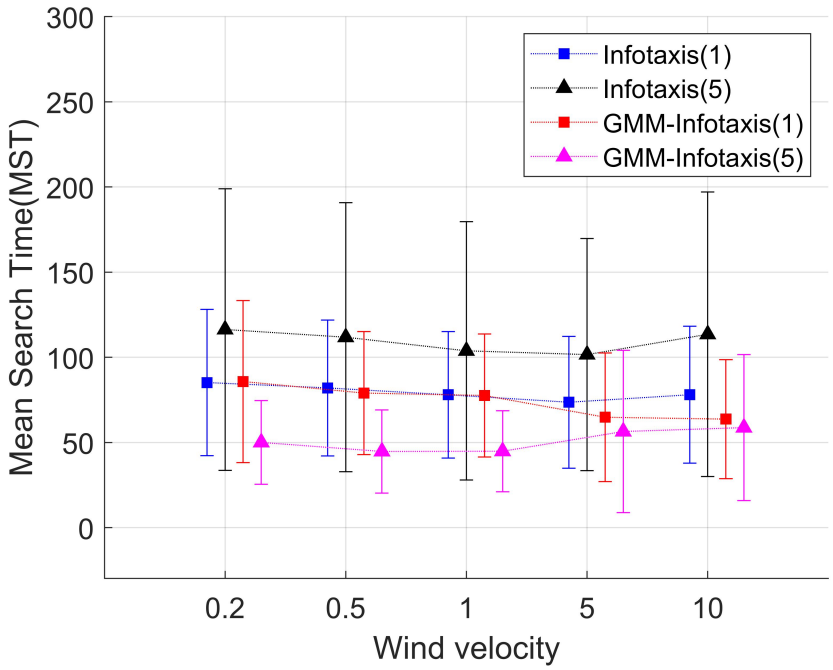

Figure 10: MST with different wind velocities and movement step sizes.

term much more efficiently when the movement step size is large.

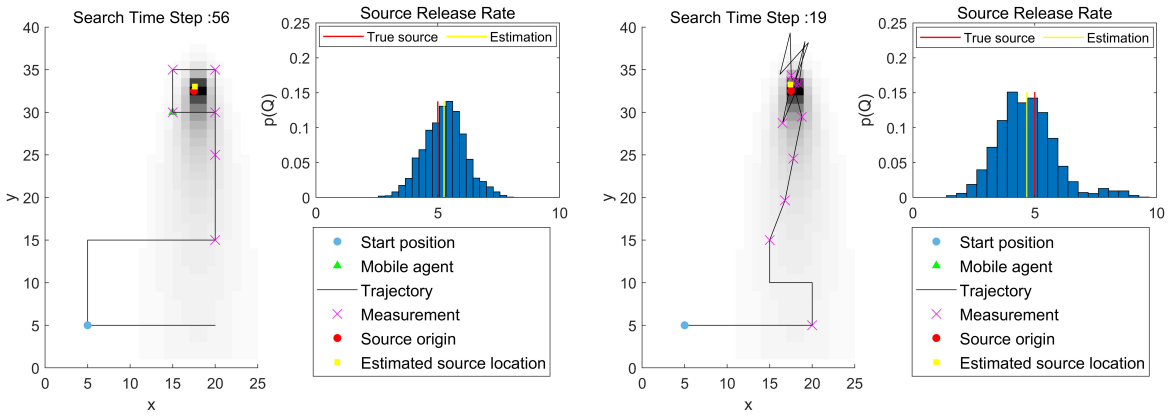

(a) Search path of Infotaxis

(b) Search path of GMM-Infotaxis

Figure 11: Search path and estimated release rate of Infotaxis and GMM-Infotaxis when $Q_0 = 5$ and $V = 5$.

5.2 Experiment Setup

For the application of the proposed approach on a physical system searching for a source origin, the multirotor unmanned aerial vehicle (UAV) equipped with tVOC sensors is used as a mobile sensor. Carrying out the outdoor source search experiments in a turbulent atmosphere using the UAV is very challenging since the gas dispersion is highly affected by the wind and disturbance generated by the UAV [27]. In our experiment, the UAV flies in the outdoor environment as shown in Fig. 12 and the systematic scheme of the flight experiment is shown in Fig. 13.

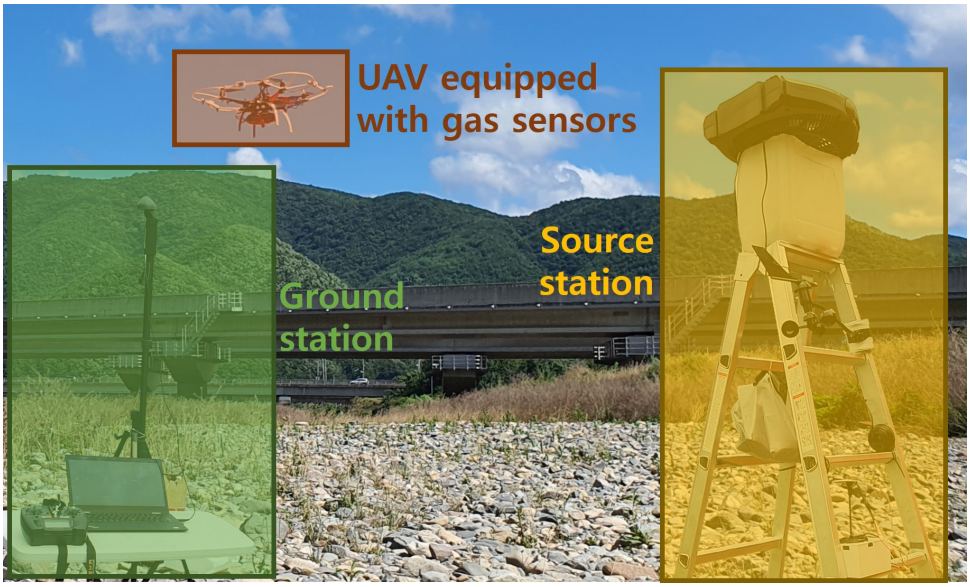

Figure 12: A snapshot of the outdoor source term estimation experiment using the UAV.

The equipment for this flight experiment is largely divided into three parts: UAV, source station, and ground station. The UAV flies autonomously to estimate the source parameters including the source location, release rate, substance lifetime, and effective diffusivity. Note that, the substance lifetime and effective diffusivity were assumed to be known as prior knowledge in the numerical simulations; however, as it is difficult to know them in the experiment, they were additionally considered as the source term estimation parameter. The source station generates a gas plume, and an anemometer is installed to measure and provide the wind direction and speed around the source. The true location of the source for verifying the experiment results is measured and transmitted to the ground station. The ground station receives various information from the UAV and source station and displays it to the human supervisor.

Environment setup

Multiple experiments are conducted with different source locations. The search area at $30 \times 30 m^2$ where the starting position (0,0) $[m]$ of the mobile sensor and the source location are indicated in Fig. 14. The source is located at $1.8m$ height to reduce the ground effect. The locations of the UAV and the source are provided by Real-Time Kinematic (RTK) GNSS.

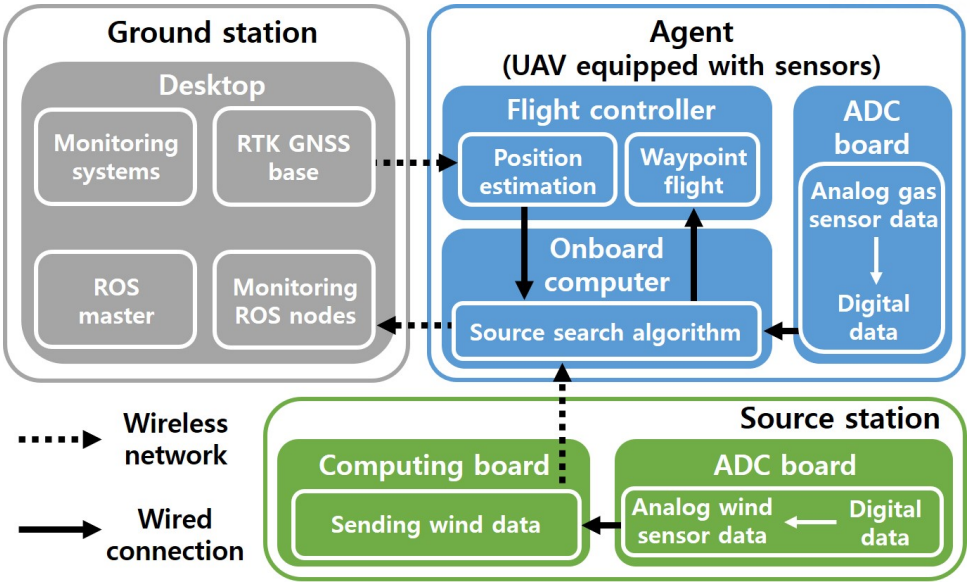

Figure 13: A systematic scheme of outdoor experiment.

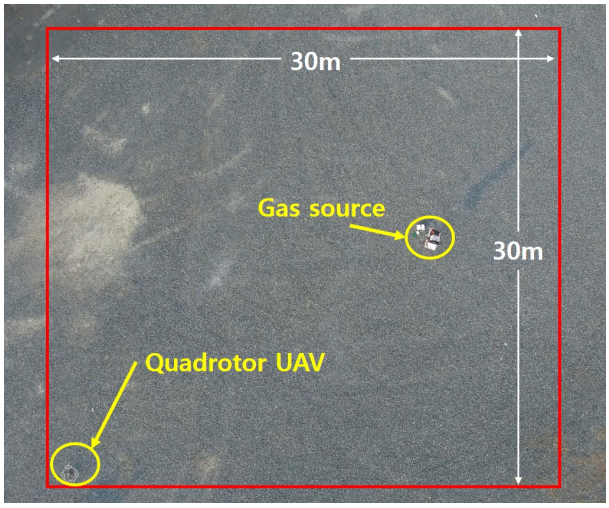

Figure 14: An example of the search area for the outdoor experiment.

The highly turbulent invisible acetone vapor generated from the source station is diffused into the atmosphere and used to simulate the hazardous gas leakage situation. The vapor is released at about $2g/s$. The silicon rubber heater maintains the temperature of the liquid acetone, and the ultrasonic humidifier and the fan are used to maintain the high release rate. The anemometer is installed next to the source to collect the wind data. The Arduino is adopted as the Analog-to-Digital Converter (ADC) to transform the analog signal type sensor data from the anemometer. The collected data including wind information and source location are gathered at the computing board and sent via a wireless network. Each part of the source station is shown in Fig. 15. If the wind direction is incorrectly estimated, the source search and estimation might be distorted. Therefore, in this study, the UAV receives and utilizes the real-time wind speed and direction with 45° intervals from the anemometer via a wireless network. An example of

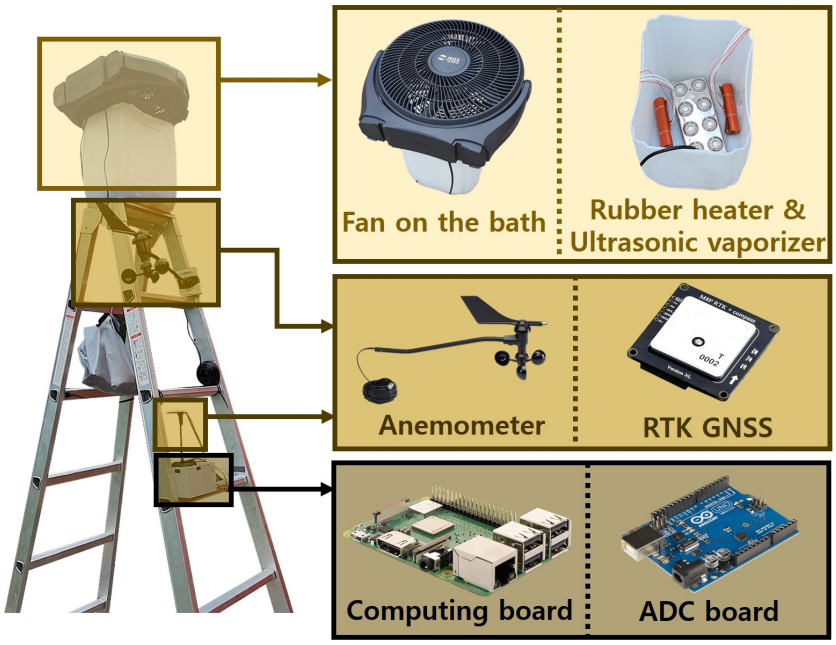

Figure 15: The source station.

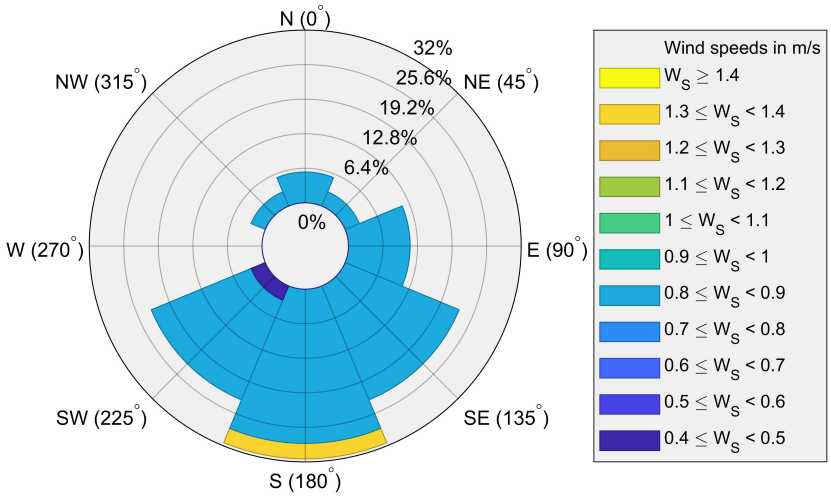

Figure 16: An example of the wind rose during a single experiment.

the changing wind currents during the experimental run by the wind rose diagram is shown in Fig. 16 [43].

Mobile agent and algorithm setup

The quadrotor UAV equipped with multiple gas sensors is used as the mobile sensor for the source search experiments as shown in Fig. 17. The on-board gas sensor, GSAS61-P110, is a semi-conductor sensor and can detect various organic solvents including acetone. The sensors are placed on different sides of the UAV to improve the response of the sensors and minimize

the wind disturbance effects by rotors.

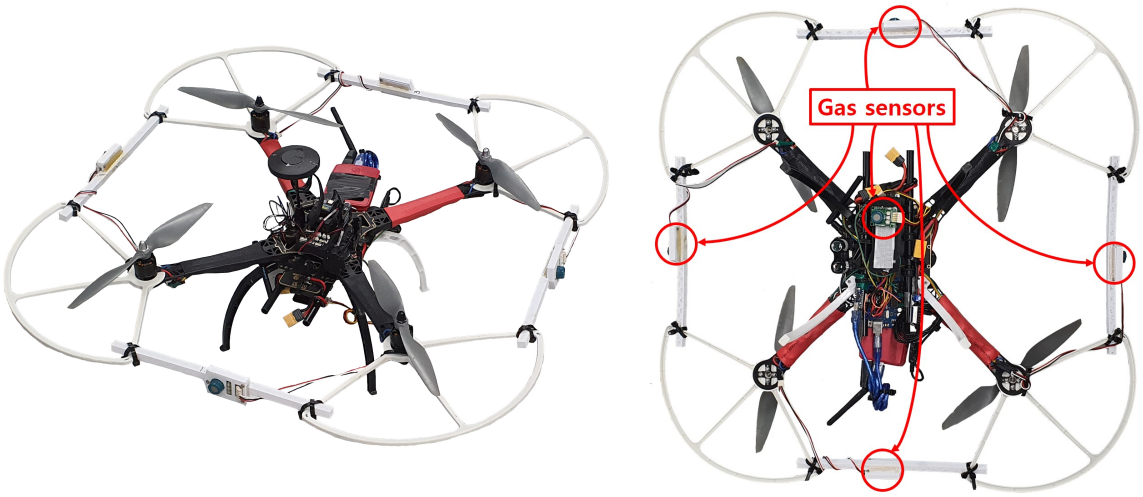

(a) Upside view (b) Downside view

Figure 17: The source search quadrotor UAV equipped with five gas sensors and the on-board computer.

In this experiment, the gas sensor measures the concentration in *ppm* which is a continuous measurement. However, the discrete particle encounter model is used as the sensor model as described in Eq. (5), which measures how many particles in the unit volume (m^3) hit the sensor [7, 44]. We assume that $10ppm$ gas concentration from the real sensor indicates the one particle contained in unit volume for the sensor model; hence, the sensor observation converts the continuous measurement values to the discrete particle encounters using $10ppm = 1particle/m^3$.

The mavlink data from the Pixhawk2 flight control unit and the gas sensor data is sent via serial communication to the Raspberry Pi 3 B+ on-board computer. The on-board computer collects the sensor data to estimate the source term and decides the next sampling position. The number of particles from the particle filter is set to $N = 1,000$, for the experiment while the number of particles in simulation was $N = 3,000$, to reduce the computational burden. As mentioned earlier, the source term which needs to be estimated by GMM-Infotaxis in the on-board computer is defined as $\theta = [\mathbf{r}_0, Q_0, D, \tau]^\mathsf{T}$, where each parameter represents 2-D true source location ($\mathbf{r}_0$), the release rate (Q_0), the effective diffusivity of the plume (D) and the substance lifetime of particles (τ), respectively. The initial prior of the source term is set as the uniform distribution presented in Table 5. The UAV moves in a 2D horizontal plane and the movement step size is $3m$ at a fixed altitude of $2.0m$. The experiment ends when the standard deviation of the estimated horizontal source location falls below a certain threshold $\sigma_t = 1.5m$, and the switching threshold for GMM-Infotaxis is $\sigma_s = 4.5m$.

Table 5: Source term parameters for experiment and initial priors

Parameter (symbol)	Initial prior [unit]
Source location (x)	$\mathcal{U}(0, 30)[m]$
Source location (y)	$\mathcal{U}(0, 30)[m]$
Release rate (Q_0)	$\mathcal{U}(0, 1000)[particle/s]$
Effective diffusivity (D)	$\mathcal{U}(0, 50)[m^2/s]$
Substance lifetime (τ)	$\mathcal{U}(0, 10000)[s]$

5.3 Experiment Results

Representative experimental result

The representative GMM-Infotaxis experimental run is conducted in the aforementioned environmental conditions. The true source locations is $\mathbf{r}_0 = [19.9m, 11.4m]^\mathsf{T}$ and the starting position of the UAV is $\mathbf{r}_1 = [0m, 0m]^\mathsf{T}$ as shown in Fig. 18. The standard deviation of the wind direction is 69.8° which indicates the wind stability [45, 46]. The estimated release rate of the source is shown in the upper side of Fig. 18. The estimated probability distribution is shown as a histogram, and the true release rate is indicated as the red dashed line while the blue solid line represents the estimated release rate. The 2-D trajectory of the UAV and estimation results are presented in the lower side of Fig. 18. At each time step, the UAV hovers at the blue dot for three seconds to collect the sensor data, updates the particle filter using the collected data, and decides the next sampling position that maximizes the reduction of the entropy. The red dots indicate the sensor measurements where the size of them shows the level of concentration. The true source location is indicated by the green square, and the potential source locations (i.e., particles) from the particle filter are represented as black dots and the gradation of particles indicates the weight of particles. The estimated mean source location is indicated by the pink star. The expected dispersion contour using the estimated source term and dispersion model is shown when the standard deviation of the potential source locations becomes below $4.5m$, as presented in Fig. 18 (b) and (c).

The behavior of the UAV for the source search experiment is very similar to that of the simulations. At the beginning of the experiment, the UAV tends to move across the wind. When the wind is changed, the UAV changes the direction accordingly as shown in Fig. 18 (a). The particles from the particle filter are decayed around the trajectory of the UAV since the source is not around the location where there is no measurement. The switching decision from the Infotaxis to GMM-action set occurs at 21^{st} time step, and large sensing cues are obtained until 31^{st} time step when the source term estimation is terminated as shown in Fig. 18 (b) and (c). The estimation error of the source location and the release rate using GMM-Infotaxis is $(\|\Delta\mathbf{r}\|, \Delta Q) = (0.322m, 682mg/s)$. The proposed approach allows generating more than one sensing position candidates in the upwind direction to find a more informative decision. As a

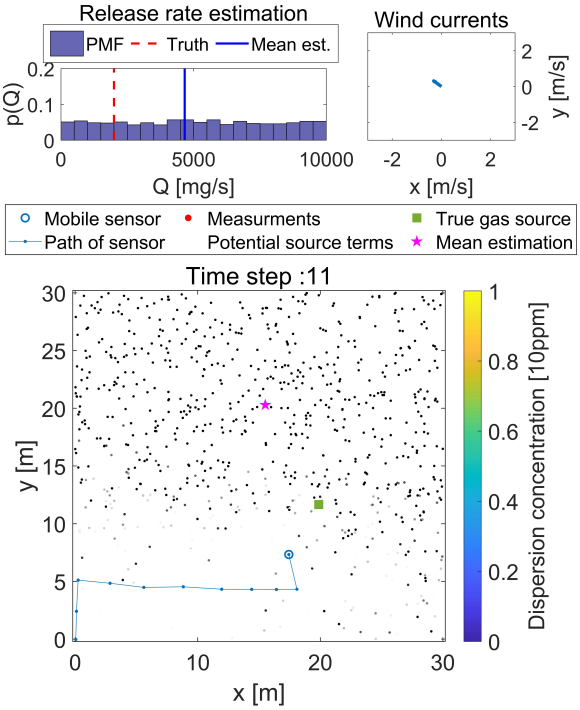

(a) At 11^{th} time step

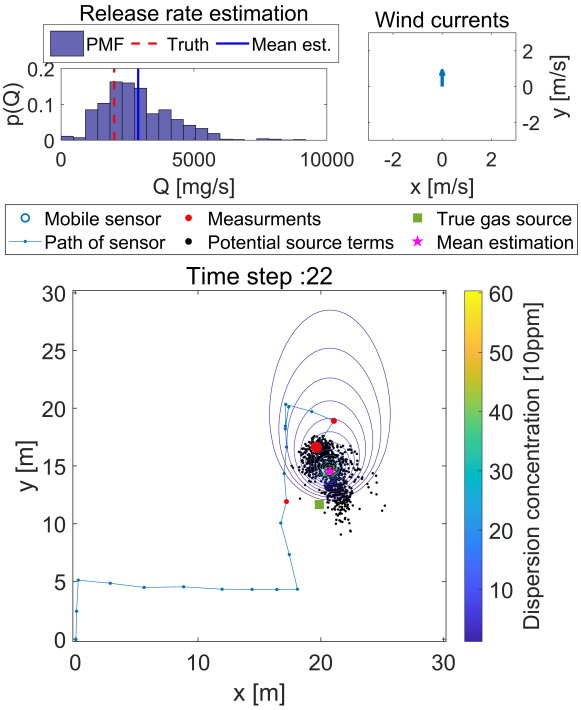

(b) At 22^{nd} time step

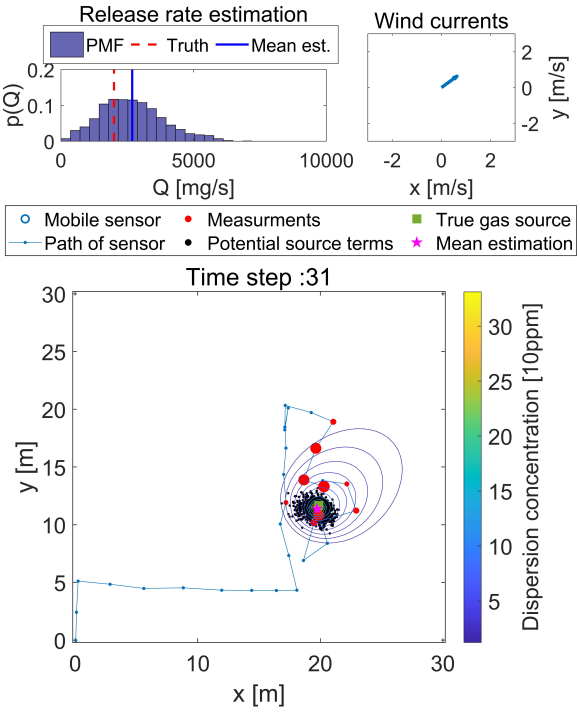

(c) At 31^{st} time step

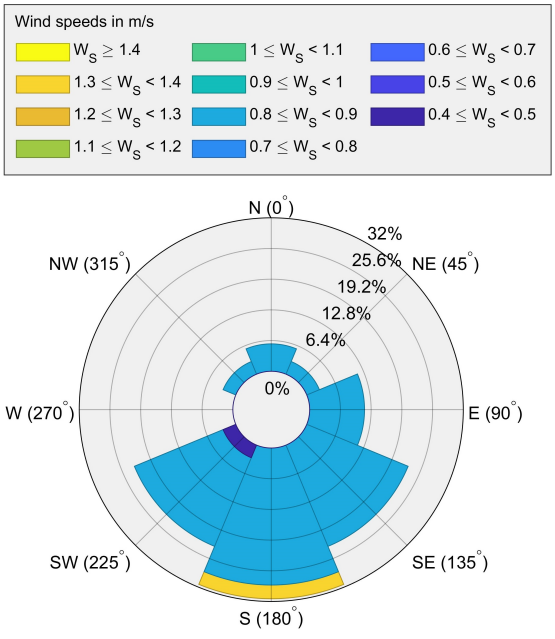

(d) Wind rose during the experiment

Figure 18: The illustrative run of experiments using GMM-Infotaxis.

Table 6: Summary of the results for multiple outdoor flight experiments

ID	Ground truth		Estimation		
	Location (x,y) [m]	Wind direction fluctuation [°]	Location (x,y) (**error**) [m]	Release rate (**error**) [mg/s]	Search time [steps]
Infotaxis					
1	(8.27,5.91)	39.6	(7.51,11.0) (**5.12**)	5231 (**3231**)	53
2	(5.03,14.8)	48.9	(0.512,14.8) (**4.52**)	1173 (**827**)	40
3	(12.2,10.7)	22.8	(12.8,13.6) (**3.04**)	209 (**1791**)	49
4	(16.1,10.5)	104	(17.7,10.2) (**1.59**)	1476 (**524**)	41
5	(5.67,19.8)	24.6	(7.72,26.4) (**6.91**)	4395 (**2395**)	49
6	(17.3,14.3)	68.1	(20.1,19.5) (**5.89**)	802 (**1198**)	52
7	(22.1,6.26)	142	(19.7,7.42) (**2.65**)	1696 (**305**)	51
8	(17.5,21.5)	146	(15.6,25.8) (**4.71**)	923 (**1077**)	33
9	(15.5,27.1)	83.7	(15.9,26.6) (**0.648**)	5194 (**3194**)	47
10	(26.7,20.5)	13.3	(27.4,17.5) (**3.02**)	1765 (**235**)	32
RMSE			(**4.24**)	(**1824**)	44.7
GMM-Infotaxis					
1	(7.07,6.66)	119	(6.87,6.73) (**0.214**)	2080 (**80**)	48
2	(14.0,8.12)	111	(15.6,7.48) (**1.76**)	1977 (**23**)	18
3	(12.3,10.8)	23.4	(12.4,10.3) (**0.537**)	2192 (**192**)	39
4	(10.8,19.1)	45.1	(10.4,19.7) (**0.680**)	1931 (**69**)	54
5	(19.9,11.7)	69.9	(19.7,11.4) (**0.322**)	2686 (**686**)	30
6	(16.0,20.8)	110	(15.7,19.3) (**1.54**)	2891 (**891**)	34
7	(6.21,25.7)	55.7	(6.26,24.9) (**0.799**)	2318 (**318**)	24
8	(26.7,6.14)	112	(28.3,6.30) (**1.63**)	2120 (**120**)	49
9	(22.0,19.4)	101	(21.7,19.6) (**0.395**)	1132 (**868**)	36
10	(26.2,25.1)	144	(25.8,23.7) (**1.54**)	1570 (**430**)	36
RMSE			(**1.10**)	(**486**)	36.8

result, sampling positions that are more suitable for converging particles can be selected in the continuous domain while maintaining the advantages of Infotaxis. In other words, by obtaining measurements at more informative positions in the continuous domain, it increases the search speed and reduces the source term estimation error.

Quantitative analysis

To demonstrate the benefit of GMM-Infotaxis over existing Infotaxis, we perform multiple outdoor experiments. The ten experiments for both Infotaxis and GMM-Infotaxis are conducted with different source locations. The other experiment conditions are the same as before. The results of both algorithms are summarized in Table 6. The RMSE, which is the root mean square error for each algorithm and is suitable for expressing precision, is provided at the last line of the table. Although the search time is highly influenced by the external environment such as atmospheric conditions, the average search time of GMM-Infotaxis is lower than that of Infotaxis. The estimation errors of the source location and release rate using the GMM-Infotaxis

method are also smaller than those of Infotaxis. This demonstrates the better search capability of GMM-Infotaxis which generates the sampling position with a higher resolution in the continuous domain. Figure 19 shows the representative runs for Infotaxis and GMM-Infotaxis among

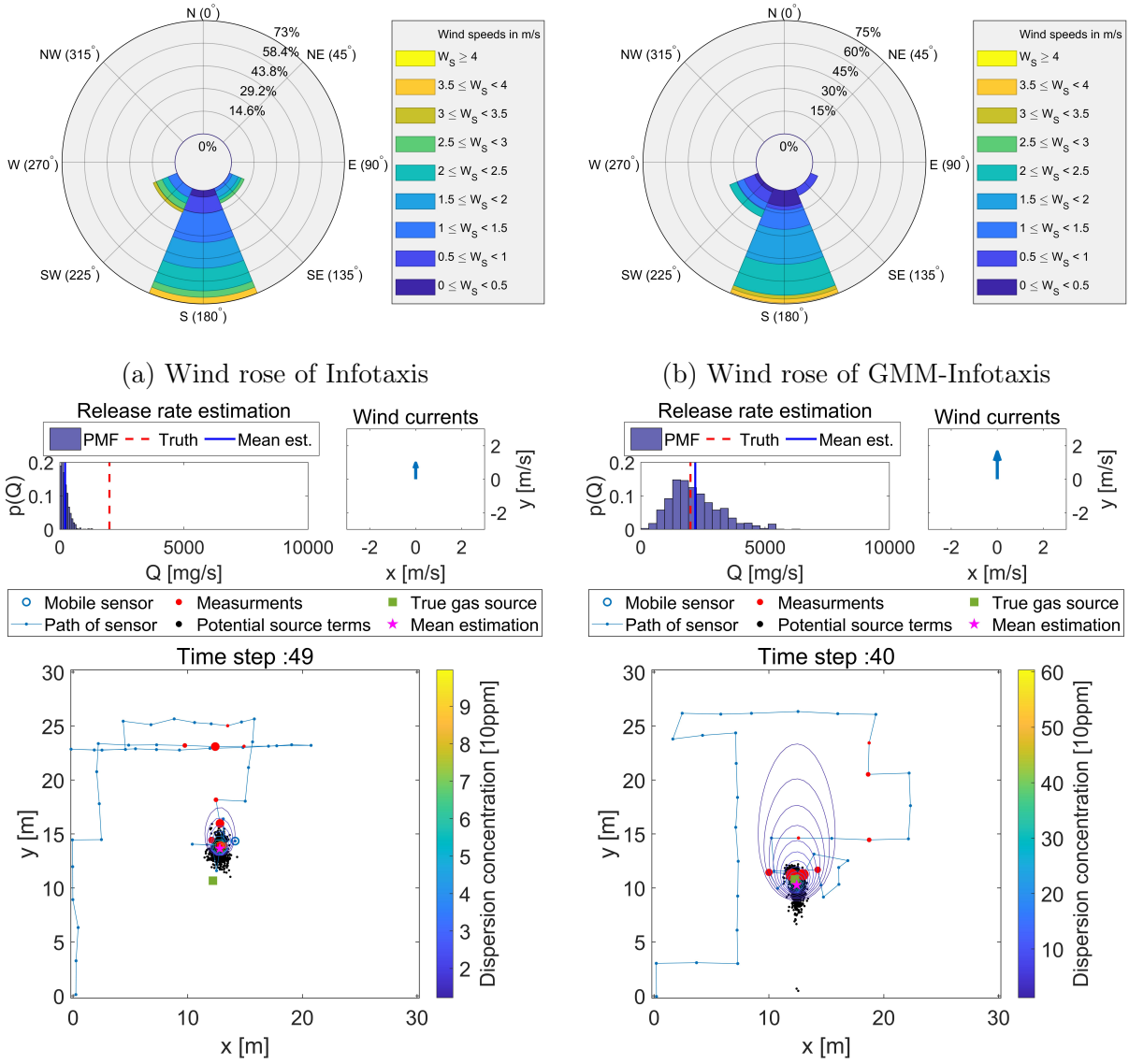

(a) Wind rose of Infotaxis

(b) Wind rose of GMM-Infotaxis

(c) Result of the Infotaxis run

(d) Result of the GMM-Infotaxis run

Figure 19: The illustrative run (ID 3 in Table 6) of experiments based on Infotaxis and GMM-Infotaxis. (a-b) show the wind rose for each experiment. (c-d) show the results of the search and estimation.

the outdoor UAV experiments presented in Table 6. Both experiments are conducted on the same day and at the same place. The wind roses during experiments are presented in Fig. 19 (a) and (b). The wind stability can be indicated by the standard deviations of the wind direction as 22.8° for Infotaxis and 23.4° for GMM-Infotaxis; thus, we can consider that experiments are conducted in a similar environment including atmospheric conditions. The UAV begins moving

along the grid nodes with $3m$ distance and when the agent collects some measurements, the particles are gathered locally. Infotaxis keeps searching among the grid nodes and it has a trouble to move toward the source limited by the grid size, but GMM-Infotaxis uses the information of the highest probable source location and move toward the true source more efficiently and accurately as shown in Fig. 19 (c) and (d). The source search and estimation are finished at 49 and 40 time steps for Infotaxis and GMM-Infotaxis, respectively. The estimation errors of the source location and the release rate using Infotaxis and GMM-Infotaxis are $(\|\Delta\mathbf{r}\|, \Delta Q) = (3.04m, 1791mg/s)$ and $(\|\Delta\mathbf{r}\|, \Delta Q) = (0.537m, 188mg/s)$, respectively.

5.4 Numerical simulations: RRT-Infotaxis

To validate the performance of the proposed RRT-Infotaxis compared with the Infotaxis [8] and GMM-Infoaxis, we performed Monte Carlo simulations in a 2-D environment. The Gaussian plume model and binary sensor model are utilized explained in Section II. As explained earlier, the use of a Gaussian sensor model requires discretizing successive measurements within a certain discrete interval for implementation. This is because it is not possible to incorporate all future measurements for the continuous area. Therefore, the discretized binary sensor model derived from discretized Gaussian sensor model is utilized in the simulation. In addition, RRT-Infotaxis aims to reduce the computational load by proposing a binary sensor model considering multi-steps. For finding the proper number of the node N_{tn} and receding horizon step (RH-step) m, corresponding numerical simulations are first conducted as these two parameters affects the performance of the algorithm. After finding the proper values, the superior performance of the RRT-Infotaxis compared with existing approaches is proven by numerical simulations in several different environments.

Gas dispersion model in an environment with obstacles

For the simulations, gas dispersion situations need to be modeled. To describe it, the Graz Lagrangian Model (GRAL), which is developed at the Graz University of Technology, Austria, is utilized for simulations computing flows around obstacles [47]. It is revised Lagrangian particle model where Lagrangian particle model produces gas particles from the diffusion source by considering not only the gas properties but also the statistical environment. This model assumes that atmospheric diffusion is able to be modeled by a Markov chain process and represents portions of each particle by calculating three-dimensional wind velocity [48]. The GRAL model is adopted as the dispersion model in the environment with obstacles as it is suitable for fast and robust modeling in a large area [47]. The example map is described in Fig. 20 and the parameters used in the example map are as follows.

- True source term: $Q_0 = 2kg/h = 0.56g/h, \mathbf{r}_0 = [197m, 235m]^\top$;
- Search area: $A = 255m \times 267m$, wind velocity $V = 2m/s$ and direction $\phi = 240°$, horizontal standard deviation $\sigma_y = 20$, vertical standard deviation $\sigma_z = 10$, stacking height $H = 11m$;
- Search agent: Movement step size $d = 9m$ and assumed it flight at $11m$ above the ground which is the same with the gas stacking height. The real senor noise $\sigma_g = R(\mathbf{r}_k|\mathbf{r}_0) + 10$;
- Estimation condition: Number of particles for the particle filter $N = 3,000$. It is assumed that the sensor noise is larger than that of the real noise, i.e., $\sigma_g = 10R(\mathbf{r}_k|\mathbf{r}_0) + 10$;
- Terminal conditions: standard deviation of the particle filter $\sigma_t = 2$, and the estimation success threshold $d_s = 2m$.

Figure 20: The example gas dispersed map with obstacles using GRAL model.

The effect receding horizon steps (RH-steps)

In an environment full of obstacles, predicting only the next step is not a good choice to efficiently choose the appropriate path for mobile agents. For instance, if the mobile agent is trapped in a corner, it is likely to move around that region or visit the same location several times. To avoid this situation, the receding horizon (RH) approach is suggested. However, as it is difficult to prove mathematically the number of optimal RH-steps, numerical simulations with different RH-steps are conducted. With changing the number of nodes, the mean search time (MST) of RRT-Infotaxis with different RH-step is compared. In Fig. 21, RH-steps from 1 to 5 is denoted as RH1, RH2, ..., RH5. When the node number increases to 30, every case except for the case RH1 shows the decreased MST. Also, it shows that increasing the number of nodes does not imply the efficiency of the algorithm. By following this result, RH3 can be seen as the proper value with 30 number of nodes. Although the MST when RH4 with 30 nodes is almost the same with that of the RH3, increasing RH-step also increases the computational load.

The effect of the new utility function

In this section, to know the effect of the new utility function, two RRT-Infotaxis with different utility functions are compared considering 3 RH-steps. RRT-Infotaxis only with the entropy utility function is denoted as $\mathbf{J}_1$ and the proposed utility function as $\mathbf{J}_1 + \mathbf{J}_2$ in the table 7 where $\mathbf{J}_1$ and $\mathbf{J}_2$ are defined in Section 4.2. By using the proposed utility function, the MST and

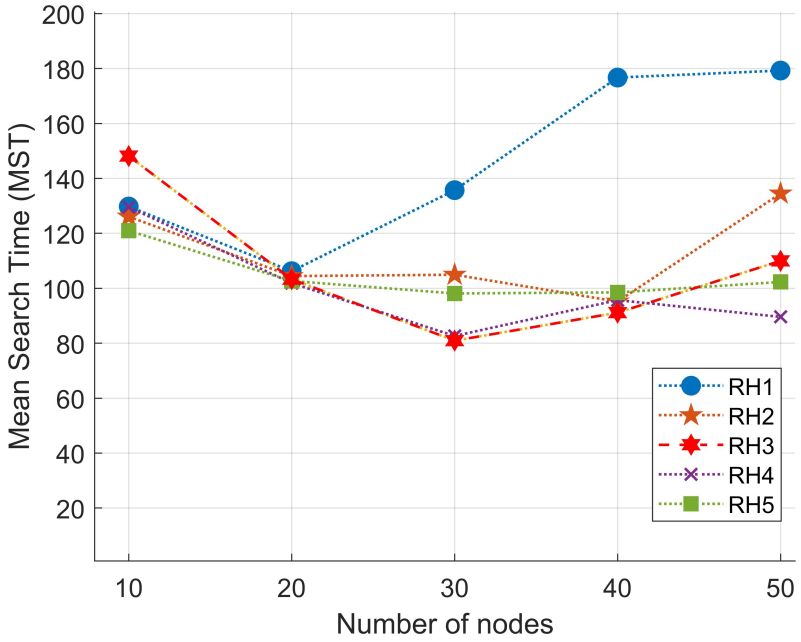

Figure 21: The MST of RRT-Infotaxis with subjected to RH-step.

standard deviation (STD) are compared in the environment described in Fig. 20 with different number of nodes.

Nodes N_{tn}	10	20	30	40	50
$\mathbf{J}_1 + \mathbf{J}_2$ (MST±STD)	136 ± 66	105 ± 55	81 ± 39	83 ± 62	98 ± 62
$\mathbf{J}_1$ (MST±STD)	139 ± 70	134 ± 57	123 ± 64	117 ± 53	135 ± 51

Table 7: The MST comparison of two different utility functions by increasing the number of nodes under 100 Monte Carlo simulations.

As shown in Table. 7, the proposed utility function shows the lower MST compared with the cases only using entropy utility function, J_1. As explained earlier in Section 4.2, the estimated source location gets closer to the actual source origin, the total utility function is mainly affected by the value of J_2. This implies that the more the mobile agent collects measurements, the more it is highly likely to move to the actual source location. Thus, the trend of the search algorithm goes to exploitation rather than exploration, resulting shorten MST. Besides, when the node number is 30, proposed approach shows the best performance. As the nodes are randomly generated in the specific area with a fixed radius around the current mobile agent, just a large number of nodes does not mean that it generates meaningful route (i.e., tree) for the mobile agent. Hence, in this thesis, the number of total nodes, N_{tn}, and RH-step, m, are selected as 30 and 3, respectively for the following simulations.

Simulation environments

The RRT-Infotaxis is compared with the conventional Infotaxis and GMM-Infotaxis. The mean search time (MST) and success rate (SR) are the comparison metric. Four simulation environments are designed with GRAL and illustrated in Fig. 22. In each environment, 100 Monte Carlo simulation are conducted. To design simulation environments, the configurations of the obstacles in case 3 and case 4 are designed as done in [49]. In [49], the urban environment is characterized by three parameters: α_0 - ratio of the built-up land area to the total land area, β_0 - the mean number of buildings per unit area , and γ_0 - a scale factor that describes the building height. In this thesis, as simulations are conducted in a 2-dimensional area, the height of building is assumed as the same height but higher than UAV flight altitude. Thus, in case 3, α_0 is set as 0.3 and β_0 is 100. In case 4, α_0 is also 0.3 and β_0 is defined as 150. The parameters for modeling the gas dispersion in each environment are as follows, and the other parameters are the same as described in the example map in the previous section:

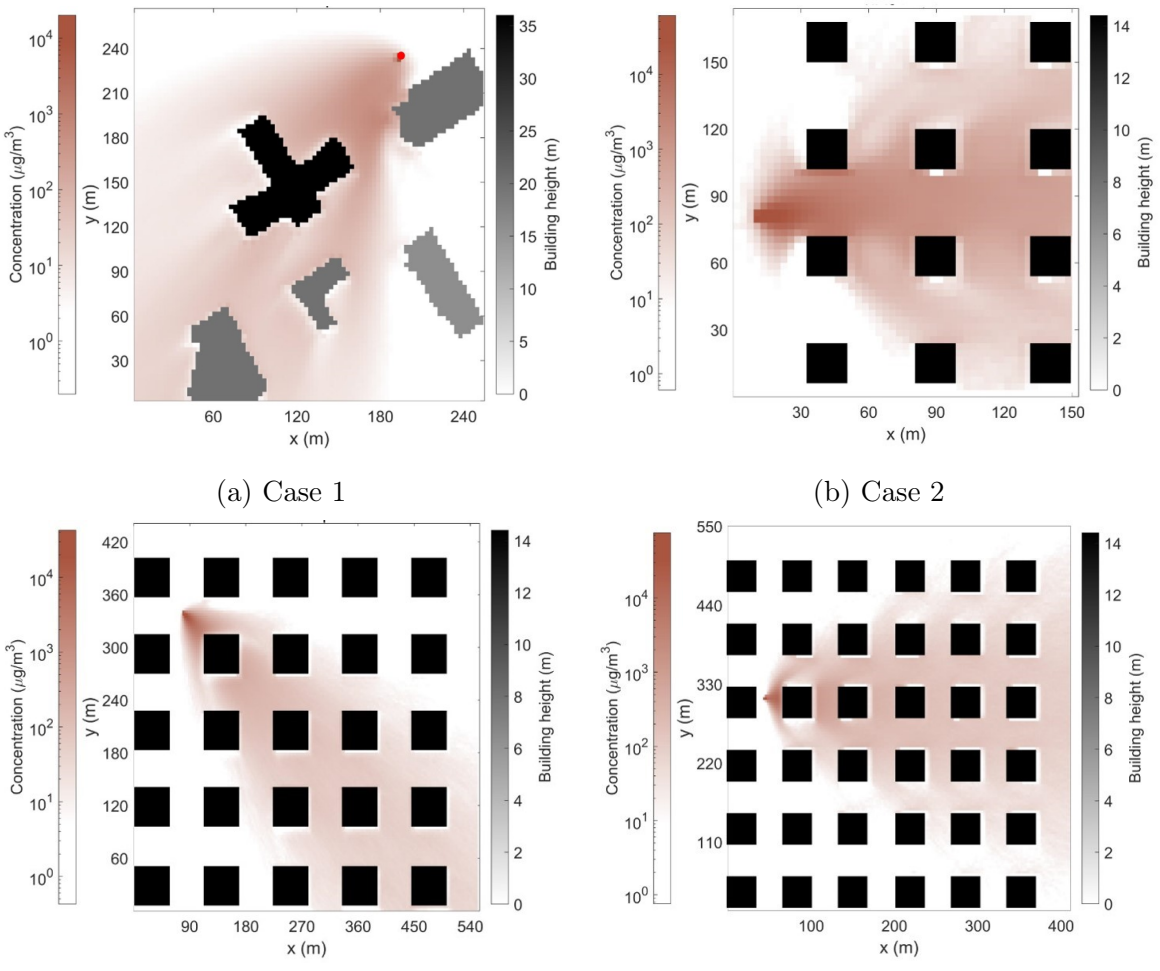

(a) Case 1

(b) Case 2

(c) Case 3

(d) Case 4

Figure 22: Four different simulation environments.

- Case 1:$A = 240 \times 260$, $\mathbf{r}_0 = [197m, 235m]^\top$, $Q_0 = 2kg/h$, $V = 2m/s, \theta = 240°$;
- Case 2: $A = 150 \times 200$, $\mathbf{r}_0 = [3m, 27m]^\top$, $Q_0 = 5kg/h$, $V = 2m/s, \theta = 0°$;
- Case 3: $A = 540 \times 420$, $\mathbf{r}_0 = [26.5m, 112.7m]^\top$, $Q_0 = 6kg/h$, $V = 5m/s, \theta = 300°$;
- Case 4: $A = 440 \times 560$, $\mathbf{r}_0 = [21m, 81m]^\top$, $Q_0 = 6kg/h$, $V = 2m/s, \theta = 0°$.

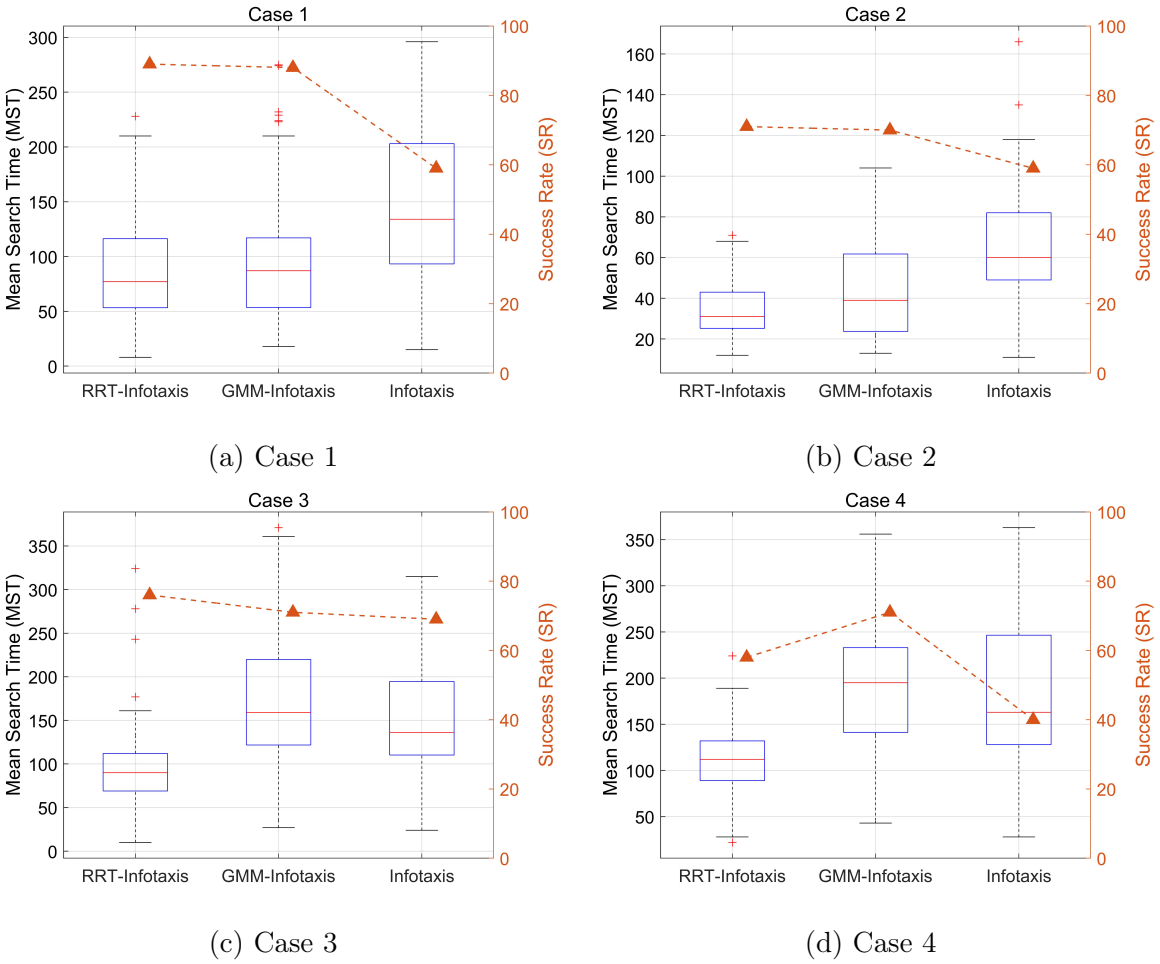

(a) Case 1 (b) Case 2

(c) Case 3 (d) Case 4

Figure 23: The MST comparison of RRT-Infotaxis, GMM-Infotaxis and Infotaxis in each case.

The results over 100 Monte Carlo simulations of with each case from 1 to 4 illustrated in Fig. 22 are represented in Fig. 23. From the results, RRT-Infotaxis shows the lowest MST in all cases and highest SR except the case 4, but the SR is still higher than conventional Infotaxis. It shows that generating action candidates in a continuous obstacle-free domain and receding-horizon approach with proposed utility function is able to guide the mobile agent more efficient path for the source term estimation. Note that, the MST of GMM-Infotaxis is slightly higher than that of the conventional Infotaxis in case 3 and 4. It is because the action candidates of GMM-Infotaxis is hindered by the obstacles.

VI Conclusions and Future work

An autonomous source search algorithms have been developed to decide the informative sampling position in a continuous action domain to estimate the source term of the released gas substance in the atmosphere. The particle filter is used to estimate the source term in highly non-linear and non-Gaussian environments. The Gaussian Mixture Model (GMM) is used to generate the informative sampling position candidates and the information-theoretic utility function is adopted to evaluate the amount of information that the mobile sensors can obtain at the sampling position. The switching process is introduced to improve search performance by balancing between exploration and exploitation. The simulations and outdoor flight experiments are conducted to compare the performance between Infotaxis and GMM-Infotaxis. From the results of simulations and experiments, we could conclude that the proposed GMM-Infotaxis algorithm outperforms Infotaxis in terms of search time and estimation accuracy. Since GMM-Infotaxis selects the action among the continuous action domain, it can select the sensing location more densely around the source location. This nature leads the agent to rapid search and accurate estimation. However, with the environment with obstacles, Rapidly-exploring random trees (RRT) is introduced for the source search not only to generate action candidates in a continuous domain but also to avoid obstacles. Also, new utility function combined with A* method is utilized for generating efficient source search path. Compared to the conventional Infotaxis and GMM-Inftoaxis, RRT-Infotaxis shows the lowest MST with all of the numerical simulations. It is because of taking receding horizon method which considers several steps ahead. No matter what the configurations of the obstacles are, RRT-Infotaxis is able to easily applied and new utility function plays a role as balancing exploration and exploitation.

There are several areas for future research that could improve the performance of the system or expand its capability. This study uses the steady-state dispersion model with a constant wind. However, this model may not fit the real experiment which has unstable wind conditions. Thus, a more realistic plume model could improve the estimation performance. Besides, in the experiments of GMM-Infotaxis, the anemometer is used to measure the wind data but the studies on wind direction estimation using a multirotor drone are in progress [50–52]. The wind estimation methods on-board the UAV could expand the capability of the algorithm. Finally, the experiments in this thesis were restricted to an open area without obstacles. There are more challenging environments in the real world, such as industrial or urban areas. The RRT-Infotaxis can be conducted such environment. To prove the enhanced performance of the RRT-Infotaxis, real world experiments are essential. The real mobile sensor platform should be expanded to handle those situations.

References

[1] M. Hutchinson, H. Oh, and W.-H. Chen, "A review of source term estimation methods for atmospheric dispersion events using static or mobile sensors," *Information Fusion*, vol. 36, pp. 130–148, 2017.

[2] J. A. Farrell, J. Murlis, X. Long, W. Li, and R. T. Cardé, "Filament-based atmospheric dispersion model to achieve short time-scale structure of odor plumes," *Environmental Fluid Mechanics*, vol. 2, no. 1-2, pp. 143–169, 2002.

[3] X. Chen and J. Huang, "Odor source localization algorithms on mobile robots: A review and future outlook," *Robotics and Autonomous Systems*, vol. 112, pp. 123–136, 2019.

[4] T. Lochmatter and A. Martinoli, "Tracking odor plumes in a laminar wind field with bio-inspired algorithms," in *Experimental Robotics*. Springer, 2009, pp. 473–482.

[5] V. Hernandez Bennetts, A. J. Lilienthal, P. Neumann, and M. Trincavelli, "Mobile robots for localizing gas emission sources on landfill sites: is bio-inspiration the way to go?" *Frontiers in Neuroengineering*, vol. 4, p. 20, 2012.

[6] J. R. Bourne, E. R. Pardyjak, and K. K. Leang, "Coordinated bayesian-based bioinspired plume source term estimation and source seeking for mobile robots," *IEEE Transactions on Robotics*, vol. 35, no. 4, pp. 967–986, 2019.

[7] M. Vergassola, E. Villermaux, and B. I. Shraiman, "Infotaxis as a strategy for searching without gradients," *Nature*, vol. 445, no. 7126, p. 406, 2007.

[8] B. Ristic, A. Skvortsov, and A. Gunatilaka, "A study of cognitive strategies for an autonomous search," *Information Fusion*, vol. 28, pp. 1–9, 2016.

[9] M. Hutchinson, H. Oh, and W.-H. Chen, "Entrotaxis as a strategy for autonomous search and source reconstruction in turbulent conditions," *Information Fusion*, vol. 42, pp. 179–189, 2018.

[10] M. Park and H. Oh, "Cooperative information-driven source search and estimation for multiple agents," *Information Fusion*, vol. 54, pp. 72–84, 2020.

[11] H. Hajieghrary, M. A. Hsieh, and I. B. Schwartz, "Multi-agent search for source localization in a turbulent medium," *Physics Letters A*, vol. 380, no. 20, pp. 1698–1705, 2016.

[12] M. Vergassola, E. Villermaux, and B. I. Shraiman, "'Infotaxis' as a strategy for searching without gradients," *Nature*, vol. 445, no. 7126, pp. 406–409, 2007.

[13] B. Ristic, C. Gilliam, W. Moran, and J. L. Palmer, "Decentralised multi-platform search for a hazardous source in a turbulent flow," *Information Fusion*, vol. 58, pp. 13–23, 2020.

[14] Z. Liu and T.-F. Lu, "Odor source localization in complicated indoor environments," in *2008 10th International Conference on Control, Automation, Robotics and Vision*. IEEE, 2008, pp. 371–377.

[15] Z. Z. Liu, Y. J. Wang, and T. F. Lu, "Odor source localization using multiple robots in complicated city-like environments," in *Advanced Materials Research*, vol. 291. Trans Tech Publ, 2011, pp. 3337–3344.

[16] B. Ristic, A. Skvortsov, and A. Walker, "Autonomous information driven search for a diffusive source in an unknown structured environment," in *2014 IEEE Workshop on Statistical Signal Processing (SSP)*. IEEE, 2014, pp. 296–299.

[17] ——, "Autonomous search for a diffusive source in an unknown structured environment," *Entropy*, vol. 16, no. 2, pp. 789–813, 2014.

[18] Y. Zhao, B. Chen, Z. Zhu, F. Chen, Y. Wang, and D. Ma, "Entrotaxis-jump as a hybrid search algorithm for seeking an unknown emission source in a large-scale area with road network constraint," *Expert Systems with Applications*, p. 113484, 2020.

[19] Y. Zhao, B. Chen, Z. Zhu, F. Chen, Y. Wang, and Y. Ji, "Searching the diffusive source in an unknown obstructed environment by cognitive strategies with forbidden areas," *Building and Environment*, vol. 186, p. 107349, 2020.

[20] G. Sandini, G. Lucarini, and M. Varoli, "Gradient driven self-organizing systems," in *Proceedings of IEEE/RSJ International Conference on Intelligent Robots and Systems (IROS)*, vol. 1. IEEE, 1993, pp. 429–432.

[21] P. Yao, H. Wang, and H. Ji, "Gaussian mixture model and receding horizon control for multiple uav search in complex environment," *Nonlinear Dynamics*, vol. 88, pp. 903–919, 2017.

[22] S. A. A. Shahidian and H. Soltanizadeh, "Path planning for two unmanned aerial vehicles in passive localization of radio sources," *Aerospace Science and Technology*, vol. 58, pp. 189–196, 2016.

[23] J. Karimi and S. H. Pourtakdoust, "Optimal maneuver-based motion planning over terrain and threats using a dynamic hybrid pso algorithm," *Aerospace Science and Technology*, vol. 26, no. 1, pp. 60–71, 2013.

[24] Y. Liu, X. Zhang, X. Guan, and D. Delahaye, "Adaptive sensitivity decision based path planning algorithm for unmanned aerial vehicle with improved particle swarm optimization," *Aerospace Science and Technology*, vol. 58, pp. 92–102, 2016.

[25] M. S. Arulampalam, S. Maskell, N. Gordon, and T. Clapp, "A tutorial on particle filters for online nonlinear/non-gaussian bayesian tracking," *IEEE Transactions on Signal Processing*, vol. 50, no. 2, pp. 174–188, 2002.

[26] C. Song, Y. He, B. Ristic, and X. Lei, "Collaborative infotaxis: Searching for a signal-emitting source based on particle filter and gaussian fitting," *Robotics and Autonomous Systems*, vol. 125, p. 103414, 2020.

[27] L. Marques, "Good experimental methodologies for mobile robot olfaction," in *Proc. Robot., Sci. Syst. Conf.(RSS)*, vol. 28, 2011, pp. 291–294.

[28] K. S. Eu and K. M. Yap, "Chemical plume tracing: A three-dimensional technique for quadrotors by considering the altitude control of the robot in the casting stage," *International Journal of Advanced Robotic Systems*, vol. 15, no. 1, p. 1729881418755877, 2018.

[29] P. P. Neumann, V. Hernandez Bennetts, A. J. Lilienthal, M. Bartholmai, and J. H. Schiller, "Gas source localization with a micro-drone using bio-inspired and particle filter-based algorithms," *Advanced Robotics*, vol. 27, no. 9, pp. 725–738, 2013.

[30] M. Hutchinson, P. Ladosz, C. Liu, and W.-H. Chen, "Experimental assessment of plume mapping using point measurements from unmanned vehicles." in *2019 International Conference on Robotics and Autonomous*, 2019.

[31] M. Hutchinson, C. Liu, and W.-H. Chen, "Information-based search for an atmospheric release using a mobile robot: Algorithm and experiments," *IEEE Transactions on Control Systems Technology*, vol. 27, no. 6, pp. 2388–2402, 2018.

[32] X. He, J. A. Steiner, J. R. Bourne, and K. K. Leang, "Gaussian-based kernel for multi-agent aerial chemical-plume mapping," in *Dynamic Systems and Control Conference*, vol. 59162. American Society of Mechanical Engineers, 2019, p. V003T21A004.

[33] J. A. Steiner, J. R. Bourne, X. He, D. M. Cropek, and K. K. Leang, "Chemical-source localization using a swarm of decentralized unmanned aerial vehicles for urban/suburban environments," in *Dynamic Systems and Control Conference*, vol. 59162. American Society of Mechanical Engineers, 2019, p. V003T21A006.

[34] M. Hutchinson, C. Liu, and W.-H. Chen, "Source term estimation of a hazardous airborne release using an unmanned aerial vehicle," *Journal of Field Robotics*, vol. 36, no. 4, pp. 797–817, 2019.

[35] I. Senocak, N. W. Hengartner, M. B. Short, and W. B. Daniel, "Stochastic event reconstruction of atmospheric contaminant dispersion using bayesian inference," *Atmospheric Environment*, vol. 42, no. 33, pp. 7718–7727, 2008.

[36] S. Chakraborty, "Generating discrete analogues of continuous probability distributions-a survey of methods and constructions," *Journal of Statistical Distributions and Applications*, vol. 2, no. 1, p. 6, 2015.

[37] B. Ristic, S. Arulampalam, and N. Gordon, *Beyond the Kalman filter: Particle filters for tracking applications*. Artech house, 2003.

[38] S. Thrun, W. Burgard, and D. Fox, *Probabilistic robotics*. MIT press, 2005.

[39] U. Orguner and M. Demirekler, "Maximum likelihood estimation of transition probabilities of jump markov linear systems," *IEEE Transactions on Signal Processing*, vol. 56, no. 10, pp. 5093–5108, 2008.

[40] J. Park and H. Baek, "Stereo vision based obstacle collision avoidance for a quadrotor using ellipsoidal bounding box and hierarchical clustering," *Aerospace Science and Technology*, vol. 105882, pp. 1–19, 2020.

[41] S. M. LaValle, "Rapidly-exploring random trees: A new tool for path planning," 1998.

[42] P. Hart, N. Nilsson, and B. Raphael, "A formal basis for the heuristic determination of minimum cost paths," *IEEE Transactions on Systems Science and Cybernetics*, vol. 4, no. 2, pp. 100–107, 1968. [Online]. Available: https://doi.org/10.1109/tssc.1968.300136

[43] U. Saha, S. Talukdar, S. Jana, and A. Maitra, "Effects of air pollution on meteorological parameters during deepawali festival over an indian urban metropolis," *Atmospheric Environment*, vol. 98, pp. 530–539, 2014.

[44] B. I. Shraiman and E. D. Siggia, "Scalar turbulence," *Nature*, vol. 405, no. 6787, pp. 639–646, 2000.

[45] J. L. Woodward, *Estimating the flammable mass of a vapor cloud*. John Wiley & Sons, 2010, vol. 21.

[46] L. Vervecken, J. Camps, and J. Meyers, "Accounting for wind-direction fluctuations in reynolds-averaged simulation of near-range atmospheric dispersion," *Atmospheric Environment*, vol. 72, pp. 142–150, 2013.

[47] D. Oettl, "Evaluation of the revised lagrangian particle model gral against wind-tunnel and field observations in the presence of obstacles," *Boundary-Layer Meteorology*, vol. 155, no. 2, pp. 271–287, 2015.

[48] M. Uliasz, "Lagrangian particle dispersion modeling in mesoscale applications," *SMR*, vol. 760, p. 23, 1994.

[49] P. Ladosz, H. Oh, G. Zheng, and W.-H. Chen, "Gaussian process based channel prediction for communication-relay uav in urban environments," *IEEE Transactions on Aerospace and Electronic Systems*, vol. 56, no. 1, pp. 313–325, 2019.

[50] R. T. Palomaki, N. T. Rose, M. van den Bossche, T. J. Sherman, and S. F. De Wekker, "Wind estimation in the lower atmosphere using multirotor aircraft," *Journal of Atmospheric and Oceanic Technology*, vol. 34, no. 5, pp. 1183–1191, 2017.

[51] M. Marino, A. Fisher, R. Clothier, S. Watkins, S. Prudden, and C. S. Leung, "An evaluation of multi-rotor unmanned aircraft as flying wind sensors," *International Journal of Micro Air Vehicles*, vol. 7, no. 3, pp. 285–299, 2015.

[52] C. Brosy and H. Kunstmann, "Simultaneous multicopter-based air sampling and sensing of meteorological variables," 2017.

Acknowledgements

This thesis becomes a reality with the kind support and help of many individuals. I would like to extend my sincere thanks to all of them.

First and foremost, I would sincerely thank my thesis advisor Prof. Hyondong Oh. He is the associate professor in Department of Mechanical Engineering at UNIST. I really appreciate his instruction on the research as well as his kindness for guiding me during my Master's course. Whenever I ran into troubles, he never gave me up and helped consistently keep going in the right direction. He is always willing to help all the lab members with full of passion.

I also would like to express my gratitude to all of the members of the *Autonomous systems laboratory* at UNIST: Gangik Cho, Minkyu Park, Yeongho Song, Phong Nguyen Ngo, Bumsu Park, Dongmin Shin, Seungho Back, Minwoo Kim, Jinwoo Oh, Minjae Jung, Joonwon Choi, Geunsik Bae, Jaemin Seo, Geunsoo Kim, Heejung Shin and Dr. Xuan-toa Tran, Dr. Pawel Ladosz. They always motivated and encouraged me to keep working on my research. I would not have accomplished non of this research without you. Especially, I want to say very "Thank you" to Minkyu Park and Jaemin Seo for helping experiments no matter what the weather was hot or cold. Were it not for your help, I could not have finished experiments successfully.

Finally, I would like to say that I really appreciate my family for the encouragement. During Master's course, my mother is always by my side when times I want to rely on and she always supports not to fall down. My little sister always becomes my pleasure and gives me fuel to deal with many harsh situations. Without them, I would not have achieved any accomplishment so far.